AD-A165 843 MONTE CARLO ANALYSIS OF QUANTUM TRANSPORT AND FLUCTUATIONS IN SEMICONDUCTORS(U) MODENA UNIV (ITALY) C JACOBONI 18 FEB 86 R/D-4260-EE DAJA45-83-C-0039 1/2

UNCLASSIFIED F/G 20/12 NL

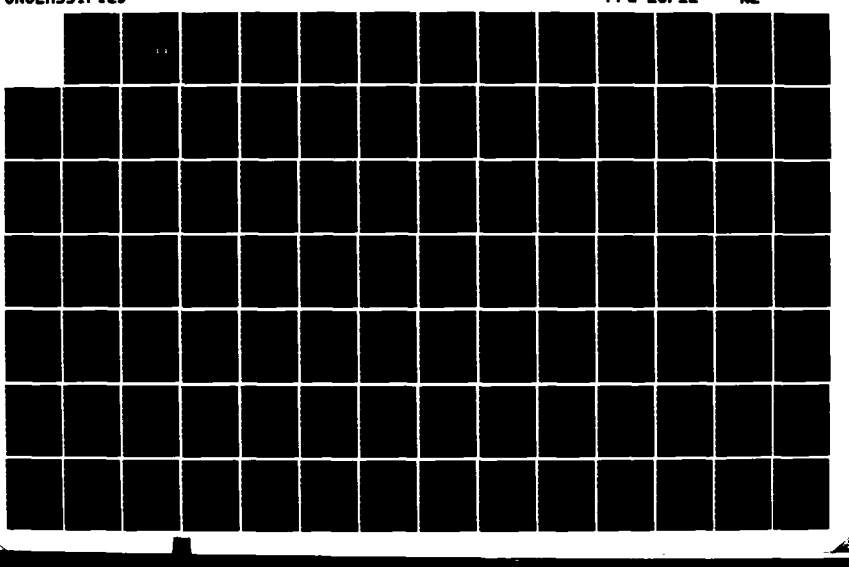

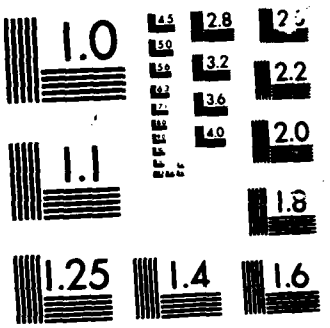

MICROCOPY RESOLUTION TEST CHART

R&D 4260-EE

(3)

ata Entered)

AD-A165 843

IN PAGE

READ INSTRUCTIONS BEFORE COMPLETING FORM	
2. GOVT ACCESSION NO.	3. RECIPIENT'S CATALOG NUMBER

4. TITLE (and Subtitle) Monte Carlo Analysis of Quantum Transport and Fluctuations in Semiconductors	5. TYPE OF REPORT & PERIOD COVERED Final Technical Report Apr 83 - Jul 85
	6. PERFORMING ORG. REPORT NUMBER
7. AUTHOR(s) Prof. Carlo Jacoboni	8. CONTRACT OR GRANT NUMBER(s) DAJA45-83-C-0039
9. PERFORMING ORGANIZATION NAME AND ADDRESS Universita Degli Studi di Modena Via G. Campi, 213/A 41100 Modena, Italy	10. PROGRAM ELEMENT, PROJECT, TASK AREA & WORK UNIT NUMBERS 61102A 1T161102BH57-03
11. CONTROLLING OFFICE NAME AND ADDRESS USARDSG-UK Box 65, FPO NY 09510-1500	12. REPORT DATE February 18, 1986 13. NUMBER OF PAGES 139
14. MONITORING AGENCY NAME & ADDRESS(if different from Controlling Office)	15. SECURITY CLASS. (of this report) Unclassified 15a. DECLASSIFICATION/DOWNGRADING SCHEDULE

16. DISTRIBUTION STATEMENT (of this Report)

Approved for Public Release; distribution unlimited

DTIC ELECTE MAR 26 1986 S D

17. DISTRIBUTION STATEMENT (of the abstract entered in Block 20, if different from Report)

18. SUPPLEMENTARY NOTES

19 KEY WORDS (Continue on reverse side if necessary and identify by block number)

Monte Carlo; Charge Transport; Quantum Transport; Fluctuations; Semiconductor Physics; Master Equation; Boltzmann Equation; Langevin Equation; Green Functions; Wigner Function; Drift Velocity; Mean Energy; Stationary Regimes; Transient Re- →

20. ABSTRACT (Continue on reverse side if necessary and identify by block number)

The present report contains technical matter related to the research performed on two different subjects. The first part concerns with quantum transport in semiconductors. A unified review of the work already published in the literature is given together with some attempts to generalize Monte Carlo methods →

DD FORM 1 JAN 73 1473 EDITION OF 1 NOV 65 IS OBSOLETE

UNCLASSIFIED

SECURITY CLASSIFICATION OF THIS PAGE (When Data Entered)

DTIC FILE COPY

86 3 25 108

19-(continuation)

gimes', Diffusivity', Autocorrelation Functions, Relaxation effects, Electron-electron Interaction.

20-(continuation)

to quantum transport within the Liouville formulation. The second part concerns with fluctuations of carrier velocities and energies both in stationary and transient regime, described by means of the correlation-function method. An analysis of the results, obtained through a Monte Carlo procedure, for covalent and polar materials yields a deep physical picture of the effect of the scattering mechanisms (phonon and carrier-carrier interactions) on the transport properties.

MONTE CARLO ANALYSIS OF QUANTUM TRANSPORT AND FLUCTUATIONS IN SEMICONDUCTORS

Final Technical Report on Contract number DAJA45-83-C-0039

Principal Investigator: Prof.Carlo Jacoboni

Performed for: European Research Office

With the collaboration of Prof. Lino Reggiani

Dr. Paolo Lugli

Dott. Rossella Brunetti

Table of Contents

1. INTRODUCTION

The present report contains technical matter related to the research performed at the Department of Physics of the University of Modena for the Contract number DAJD45/83/C/0039 "Monte Carlo analysis of quantum transport and fluctuations in semiconductors". The subject is treated at three different levels.

a) Part of the research has reached definite conclusions; in this case the material is well-organized and new results are presented. This the case of the work performed on fluctuations and on the effect of electron-electron (e-e) interaction on energy relaxation (Chapter 4).

b) Part of the research is still under development and the related material is still in the form of models and proposals. This is the case of the research devoted to the attempt to extend the Monte Carlo method to the solution of quantum transport problems (Chapter 3).

c) Part of the material contains a review of known results already present in the literature. We felt useful to perform this investigation and to present it in a unified way in order to make clear the scenario in which our research is

placed and the technical knowledge necessary for future developments (Chapter 2).

In particular this report is organized as follows. The formal quantum transport theory is reviewed in Chapter 2. Different approaches to quantum transport such as the Master Equation, the Generalized Langevin Equation, the Green function method and the Wigner function method are described and compared in their merits and shortcomings.

Chapter 3 contains the description of the attempts made to generalize Monte Carlo methods to quantum transport within the Liouville formulation. A method is propcsed to solve integro-differential equations of the type obtained in transport theories. The application of the method to the actual equations governing the motion of electrons in the presence of external and phonon fields is still under development (Section 3.4).

The research performed on fluctuations of carrier velocities and energies is described in Chapter 4. In particular Sect. 4.1 deals with the autocorrelation of velocity fluctuations, noise and diffusion in steady-state conditions, while Sect. 4.2 describes the same quantities in the transient regime. The effect of carrier-carrier

interaction is analized in the final section 4.3.

2. FORMAL THEORY OF QUANTUM TRANSPORT

2.1 Introductory Remarks

In the domain of ultrasmall structures (submicrometer) and ultrafast times (subpicosecond) simple arguments based on the uncertainty principle show that hot-electron transport in semiconductors needs a more exact approach than that offered by the semiclassical Boltzmann equation. Table 2.1 reports the various levels of description of nonequilibrium statistical mechanics. Starting from the microscopic level, identified by the Liouville von Neumann equation for the density matrix of the whole system (electrons plus scattering centers), the kinetic level describing the time evolution of the electron system can be achieved. Then, by introducing several approximations, the semiclassical Boltzmann equation can be, for example, obtained.

Theoretical efforts towards more exact quantum approaches have indeed predicted new phenomena /2.1/. Among these, the intra-collisional field effect (ICFE) and the collisional broadening (see Table 2.2) have attracted most of the researchers' attention.

The former accounts for the fact that the scattering occurs between electron states in the presence of an electric field. The latter is correlated with the finite lifetime of the electron states as a result of collisions. The main consequence of both effects is in the expectation of a smoothing in the sharp peaks of the scattering rates occurring at threshold energies, as depicted in Table 2.2. An illustrative description of the above effects, as compared with the semiclassical Boltzmann picture, is offered in Figs. (2.1-3).

Within the semiclassical Boltzmann picture (see Fig. (2.1)), an electron performs a classical trajectory in real space between successive collisions, which are treated as point-like events in space and time. Transitions between initial $\vec{k}$ and final $\vec{k}'$ wavevectors are also point like, and the well defined correspondence between $\vec{k}$ and $\epsilon(\vec{k})$ enables a straightforward calculation of the energy involved. As a result of this picture, the transition rate $P(\vec{k},\vec{k}')$ is proportional to an energy conserving delta function.

In presence of ICFE the concept of "duration of a collision" /2.2/ can be usefully introduced (see Fig. 2.2). Accordingly, a collision sphere in real space, with radius r_c

$\cong \frac{\hbar q \tau_c}{m}$ (q being the transferred wavevector $|\vec{k}-\vec{k}'|$ and τ_c the duration of the collision) can be defined /2.3/. In this way, the carrier can gain or loose energy from the field during the collision. Thus, owing to the interference between the field and the scattering mechanisms and the possible gain of energy during the collision, a scattering event can occurr which in the point-like collision model was forbidden by the energy conservation. As a result of this picture, the original energy conserving delta function is transformed in a more complicate expression (see Fig. 2.2), which can be analyzed in terms of Fresnel integrals /2.3/.

Collisional broadening is linked to the manybody nature of the phenomena. The quasi-particle approximation must be released, and a complex self-energy $\Sigma(\vec{k},\epsilon)$ has to be introduced (see Fig. 2.3). As well known /2.4/, the real part of Σ renormalizes the energy of the electron state, while the immaginary part, through the optical theorem, gives the scattering rate. Energy and wavevector are now two independent variables and a spectral density, $S(\vec{k},\epsilon)$, giving the probability of finding the electron with $(\vec{k},\epsilon)$ must be introduced. As a result of this picture, the

original energy conserving delta function is substituted by Lorentzian structures.

Different lines of approach can be pursued to establish quantum kinetic equations able to describe the above phenomena /2.5/. The aim of this chapter is to present the main results which, to the authors opinion, have recently appeared in the literature in an attempt to evidence merits and shortcomings of different formal theories. Our hope is to obtain indications on approaches which are most appropriate for numerical solutions, having in mind the possibility of extending to a quantum mechanical framework the traditional Monte Carlo technique /2.6/.

The chapter is organized as follows. Section 2.2 will specify the physical model. Sections 2.3 to 2.6 will survey the four main lines of development of the formal theory. Applications and results will be reported in Section 2.7.

2.2 The Model

We concentrate on a simple case, yet without any loss of generality, which corresponds to an ensemble of independent electrons. These electrons are under the influence of an applied electric field $\vec{E}$ which, if not otherwise stated, is taken as homogeneous in space and independent of time, and they interact with a phonon bath. Thus the total Hamiltonian of the system is partioned as:

$$H = H_e + H_F + H_P + H_{e\text{-}P} \qquad (2.1)$$

where H_e refers to electrons H_F to the electric field, H_p to the phonons and $H_{e\text{-}p}$ to the electron-phonon interaction.

As the solution of a transport problem relyes on the calculation of average values of the observables of interest (e.g. density current, concentration, energy, etc.) a prescription for such a calculation is needed. To this end different approaches can be used and, in the following, the leading ones will be surveyed.

2.3 The Generalized Master Equation

2.3.1 The Generalized Master Equation

Within a Schroedinger picture, the density matrix $\rho(t)$ of the physical system of interest is introduced. The average value at time t of an observable O, which does not depend explicitely on time, is given by:

$$\langle O \rangle_t = Tr \{ \rho(t) O \} \tag{2.2}$$

The density matrix obeys the Liouville von Neumann equation:

$$\dot{\rho}(t) = -\frac{i}{\hbar} L \rho(t) \tag{2.3}$$

$L = [H ,]$ (square brackets denote commutator) being the Liouvillian superoperator associated with H.

Following Nakaijma and Zwanzig /2.7/, irrelevant information about the electron subsystem can be eliminated through time independent projection operators. In this way, in place of Eq.(2.3), one can write a kinetic equation for the relevant part of the density matrix (generalized master

equation), which can be analyzed perturbatively in terms of the applied field and of the electron phonon interaction. Using this procedure Pottier and Calecki /2.8-10/ have introduced projection operators that allow a factorization of the density matrix for the coupled electron phonon system and they have obtained an interesting quantum kinetic equation. To restore the traslational invariance of the electron Hamiltonian in presence of a uniform electric field, they used a vector potential gauge:

$$H_e + H_F = \frac{1}{2m}\left[\vec{p} - e\vec{A}(t)\right]^2 \qquad (2.4a)$$

$$\vec{A}(t) = -\int_0^t \vec{E}(t')\,dt' \qquad (2.4b)$$

where m is the electron mass, p the momentum operator and $\vec{A}(t)$ the vector potential operator. Furthermore, statistical electron operators are introduced which at t=0 are given by:

$$Y(\vec{k},\vec{k};0) = |\vec{k}\rangle\langle\vec{k}| \qquad (2.5)$$

where time t=0 corresponds to the switching on of the field, and the $|\vec{K}\rangle$ states are the accelerated plane waves. If at $t \geq 0$ Y is evoluted by the total Hamiltonian then, to the lowest order (second) in the electron-phonon interaction, the equation of motion for $Y(\vec{K},\vec{K};t)$ is obtained:

$$\dot{Y}(\vec{K},\vec{K};t) = \int_0^t dt' \sum_{K'} \left[P(\vec{K}',\vec{K};t,t') Y(\vec{K}',\vec{K}';t') - \right.$$

$$\left. - P(\vec{K},\vec{K}';t,t') Y(\vec{K},\vec{K};t') \right] + F(\vec{K};t) \qquad (2.6a)$$

where the probabilities $P(\vec{K},\vec{K}';t,t')$ entering the integral collision term are given by:

$$P(\vec{K},\vec{K}';t,t') = \frac{2}{\hbar^2} Re \left\{ \sum_q \sum_{m=1,-1} |\langle \vec{K}| \chi_{mq} |\vec{K}'\rangle|^2 \times \right.$$

$$\times |C(\vec{q})|^2 \left(N_q + \frac{1}{2} + \frac{m}{2}\right) \exp\left[-\frac{i}{\hbar} \int_{t'}^{t} dt'' \left(\epsilon(\vec{K}' - \frac{e}{\hbar}\vec{A}(t'')) - \right.\right.$$

$$\left.\left. - \epsilon(\vec{K} - \frac{e}{\hbar}\vec{A}(t'')) + m\hbar\omega \right] \right\} \qquad (2.6b)$$

η = +1 (-1) corresponding to phonon emission (absorption)

processes. $F(\vec{K};t)$ represents a stochastic (Langevin) force which is given by:

$$F(\vec{K},t) = 2Re\left\{\frac{i}{\hbar}\sum_q C(\vec{q})\, b_q\, e^{-i\omega_q t} \sum_{K'}\right.$$

$$\left[\langle\vec{K}'|\chi_q|\vec{K}\rangle Y(\vec{K}',\vec{K};0)\, exp\left[\frac{i}{\hbar}\int_0^t dt'\left(\epsilon\left(\vec{K}'-\frac{e}{\hbar}\vec{A}(t')\right)-\epsilon\left(\vec{K}-\frac{e}{\hbar}\vec{A}(t')\right)\right]-\right.\right.$$

$$\left.\left.-\langle\vec{K}|\chi_q|\vec{K}'\rangle Y(\vec{K},\vec{K}';0)\, exp\left[-\frac{i}{\hbar}\int_0^t dt'\left(\epsilon\left(\vec{K}'-\frac{e}{\hbar}\vec{A}(t')\right)-\epsilon\left(\vec{K}-\frac{e}{\hbar}\vec{A}(t')\right)\right]\right]\right\} \tag{2.6c}$$

In contrast with the collision term, $F(\vec{K};t)$ does not involve the projections on the $|\vec{K}\rangle$ states, but only off-diagonal electron operators. In Eqs.(2.6) $C(\vec{q})$ characterizes the nature and strength of the electron phonon coupling, $\chi = \exp(i\vec{q}\cdot\vec{r})$, is the angular frequency of the phonon with wavevector $\vec{q}$, N_q is the equilibrium phonon population, $\epsilon(\vec{k})$ the eigenvalues of the zero field Hamiltonian, and $\hbar\vec{K}$ the canonical momentum given by:

$$\hbar\vec{K} = \hbar\vec{k} + e\vec{A}(t) \tag{2.6d}$$

The electron distribution function $f(\vec{K},t)$ in $|\vec{K}\rangle$ states is

conveniently expressed in the Heisenberg picture and results to be:

$$f(\vec{K},t) = Tr\left\{\rho(0)Y(\vec{K},\vec{K};t)\right\} \qquad (2.7)$$

where the trace operator acts in the whole electron phonon space.

By assuming that the initial density matrix $\rho(0)$ is factorized in the phonon and electron parts as:

$$\rho(0) = \rho_{ph}\cdot\rho_{el}(0) \qquad (2.7a)$$

one gets:

$$Tr\left\{\rho(0)\,F(\vec{K};t)\right\} = 0 \qquad (2.7b)$$

So the Langevin force does not contribute to the evolution equation of the electron distribution function. Therefore, $f(\vec{K};t)$ obeys the high field retarded transport equation:

$$\frac{\partial f(\vec{K};t)}{\partial t} = \int_0^t dt' \sum_{K'}\left\{P(\vec{K}',\vec{K};t,t')\,f(\vec{K}';t') -\right.$$

$$- P(\vec{k},\vec{k}';t,t')f(\vec{k},t')\Big\} \qquad (2.7c)$$

As merits of Eqs.(2.6): (i) a Boltzmann Langevin equation able to describe average quantities as well as fluctuations around average is obtained from first principles. (ii) An explicit microscopic expression of the random Langevin force is provided. (iii) By including the external field in the basis state, the intracollisional field effect is automatically accounted for. (iv) The choice of the vector potential gauge enables to avoid the use of the Airy functions. (v) A periodic crystal potential (Bloch electrons with interband scattering neglected) can be easily introduced.

As shortcomings: (i) Since the lowest order in the electron phonon interaction is considered, collisional broadening is not accounted for. (ii) The stationary state does not correspond to the condition that one would expect $\partial f(\vec{k},t)/\partial t = 0$.

2.3.2 Comparison Between The Generalized Master Equation And The Boltzmann Equation

To gain some physical insight, we shall compare Eq.(2.7c) with the familiar Boltzmann equation:

$$\frac{\partial f(\vec{k},t)}{\partial t} + \frac{e}{\hbar}\vec{E}\,\frac{\partial f(k,t)}{\partial \vec{k}} = \sum_{k'}\left\{P(\vec{k}',\vec{k})\,f(\vec{k}',t) - P(\vec{k},\vec{k}')\,f(\vec{k},t)\right\} \qquad (2.7d)$$

To recover Eq.(2.7d) from Eq.(2.7c) the canonical $\vec{K}$-vector has to be substituted by its expression as a function of the crystal wavevector (see Eq.(2.6d)). In doing so it is easily verified:

$$\frac{\partial}{\partial t} f(\vec{K};t) = \frac{\partial}{\partial t} f(\vec{k};t) + \frac{e}{\hbar}\vec{E}\,\frac{\partial f(k,t)}{\partial \vec{k}} \qquad (2.7e)$$

Then, by taking the ansatz of completed collisions, $\int_{t_0}^{t} \rightarrow \int_{0}^{\infty}$, in the r.h.s. of Eq.(2.7c), and neglecting the effect of the field during the collision, the collision term $P(\vec{K},\vec{K}';t,t')$ recovers the usual markovian form in the carrier wavevector representation $P(\vec{k},\vec{k}')$.

2.4 The Generalized Langevin Equation

2.4.1 The Generalized Langevin Equation

Within the Heisenberg picture, the average value of Eq.(2.2) writes:

$$\langle O \rangle_t = Tr \left\{ \rho(0)\, O_H(t) \right\} \tag{2.8}$$

where the time evolution of the operator $O_H(t)$ (here the subscript H indicates the Heisenberg picture) is given by the Heisenberg equation of motion:

$$\dot{O}_H = \frac{i}{\hbar} L\, O_H(t) \tag{2.9}$$

Following the original idea of Mori /2.11/, Zubarev /2.12/ and Grabert /2.13/ , a decomposition procedure which makes use of time-dependent projection operators can be introduced. In this way a generalized Langevin equation for the thermodinamically relevant variables (macrovariables) of the problem can be written in place of Eq.(2.7), which can be analyzed perturbatively. Following this procedure, Ferry

and coworkers /2.11-13/ have considered the set of macrovariables:

$$\{P_m\} = \{P_e, N_e, H_e, H_p, H_{e\text{-}p}\} \qquad (2.10)$$

where P is the total momentum of the electronic system, N_e the number operator of electrons and the other macrovariables are the same as in Eq.(2.1). Then, the equation of motion for the macrovariables is found to be:

$$\dot{P}(t) = exp(iLt)\,\pi(t)\,\dot{P}(0) +$$

$$+ \int_0^t ds'\, exp(iLs')\, i\pi(s')\, L\,[1-\pi(s')]\, G(s',t)\, \dot{P}(0) +$$

$$+ [1-\pi(0)]\, G(0,t)\, \dot{P}(0) - \int_0^t ds'\, exp(iLs')\, \dot{\pi}(s')\, G(s',t) \times$$

$$\times [1-\pi(t)]\, \dot{P}(0) \qquad (2.11)$$

Here $\pi(t)$ is a time dependent projection operator which is defined in terms of the chosen macrovariables and of their

average values, and the operator G(s,t) is a two time Green function given by:

$$G(s,t) = T_{-} \exp\left\{ i \int_{s}^{t} du\, L\,[1-\pi(u)] \right\} \qquad (2.12)$$

T_{-} being the Dyson time ordering operator from left to right.

The physical meaning of the terms on the r.h.s. of Eq.(2.11) can be identified in the following way. The first term gives the collisionless motion. The second term can be divided into two parts, the former characterizing the collisions and the latter leading to a fluctuating force induced by the electron-phonon interaction and the nonequilibrium nature of the system. The third and fourth terms are two additional fluctuating forces, the former being Mori like in nature and the latter characterizing the fluctuations induced by the rate of change of the macrovariables during the transient regime. The average motion of the macrovariables is determined by the equation:

$$\langle \dot{P}(t) \rangle = \langle \exp(iLt)\, \pi(t)\, \dot{P}(0) \rangle +$$

$$+ \left\langle \int_0^t ds' \exp(iLs')\,\pi(s')\,iL\left[1-\pi(s')\right] G(s',t)\,\dot{P}(0)\right\rangle \quad (2.13a)$$

As merits of Eq.(2.12): (i) A generalized Langevin equation valid at high electric fields is obtained from first principles. (ii) Separate descriptions of the motion in absence of collisions, with collisions, and with fluctuations are evidenced. (iii) Fluctuations under transient conditions are accounted for. (iv) Generalized balance equations can be obtained.

As shortcomings: (i) The choice of the pertinent macrovariables is critical but no fixed rules govern this choice, rather one must be led in doing that by physical intuition.

2.4.2 Comparison Between The Generalized Langevin Equation And The Classical Langevin Equation

To get some physical insight, a comparison of Eq.(2.11) with the classical Langevin equation and with the equation derived from first principles by Mori /2.11/, under linear response conditions, is here reported.

The Langevin equation, phenomenologically derived in presence of an electric field, takes the form:

$$\dot{\vec{p}}(t) = e\vec{E} - \frac{1}{\tau}\vec{p}(t) + R(t) \qquad (2.13b)$$

where $\vec{p}$ is the classical momentum of the particle, τ a relaxation time accounting for friction effects, and R(t) the stochastic force associated with the rapid fluctuating part of the carrier motion. A first principle justification of Eq.(2.13b) under linear response conditions in the external field was given by Mori /2.11/. By introducing a time independent projection operator Π Mori's equation for the quantum momentum P writes:

$$\dot{P}(t) = \exp(iLt)\Pi\dot{P}(0) +$$

$$+ \int_0^t ds\, \exp\left(iL(t-s)\right] \Pi i L \exp\left[i(1-\Pi)Ls\right](1-\Pi)\dot{P}(0) +$$

$$+ \exp\left[(1-\Pi)Lt\right](1-\Pi)\dot{P}(0) \qquad (2.13c)$$

where the three terms on the r.h.s. of Eq.(2.13c) are the quantum analogous of those in the r.h.s. of Eq.(2.13b). It is worth mentioning that in the Mori equation the friction term is described by a quite general retarded kernel. *Furthermore, first-principle* justification of the stochastic force, postulated by Langevin, is provided for the first time.

Under far from equilibrium conditions, the first three terms on the r.h.s. of Eq.(2.11) are the analogous of those in the r.h.s. of Eq.(2.13.c). The nonlinear condition is however responsible for the need of a time dependent projection operator and for the fourth term in Eq.(2.11). This term is related to the transient which goes from the switching on of the field, assumed to be step-like, to the stationary far-from-equilibrium condition.

2.5 The Green Function Method

2.5.1 The Green Function Method

Within a second quantized Heisenberg picture, with creation $\psi^{\dagger}(\vec{r},t)$ and annihilation $\psi(r,t)$ field operators, the average value of Eq.(2.2) writes:

$$\langle O \rangle_t = \frac{Tr\left\{ exp\left[-\beta(H_o - \mu N_e)\right] U^{-1}(t)\, O\, U(t)\right\}}{Tr\left\{ exp\left[-\beta(H_o - \mu N_e)\right]\right\}} \qquad (2.14)$$

where the average is performed on the grand canonical equilibrium ensemble (i.e. $H_o = H - H_F$, $\beta = 1/(K_B T)$, K_B being the Boltzmann constant and T_e the bath temperature, μ is the chemical potential). All the dependence of the external field is esplicitated in the evolution operator:

$$U(t) = T_+ \left\{ exp\left[-\frac{i}{\hbar} \int_{-\infty}^{t} dt' \int d\vec{r}\; \psi^{\dagger}(\vec{r},t')\, \psi(\vec{r},t')\, H_F \right] \right\} \qquad (2.15)$$

T_+ being the time order operator from right to left. Following Kadanoff and Baym /2.17/, a set of real time Green functions is introduced as:

$$G^{>}(\vec{r},t;\vec{r}',t') = -i \langle \psi(\vec{r},t)\, \psi^{\dagger}(\vec{r}',t') \rangle \qquad (2.16a)$$

$$G^{<}(r,t;r',t') = i \langle \psi^{\dagger}(\vec{r}',t')\, \psi(\vec{r},t) \rangle \qquad (2.16b)$$

where $>$ $<$ indicate $t > < t'$, respectively. The average in Eq.(2.14) can be calculated in terms of $G^{>}$ and $G^{<}$. In particular for the density current it is:

$$\langle \vec{j}(\vec{r},t) \rangle = \left\{ \frac{1}{2mh} \left(\nabla_{\vec{r}} - \nabla_{\vec{r}'} \right) G^{<}(\vec{r},t;\vec{r}',t) \right\}_{\vec{r}=\vec{r}'} \qquad (2.17)$$

On this basis, Wilkins and coworkers /2.18-20/ have developed a Generalized Kadanoff-Baym (GKB) formalism which allows to treat the external field exactly. Conceptually the calculations split into two steps. First, the motion in absence of collisions, but in presence of an electric field is treated exactly. This leads to the introduction of field dependent Green functions $G_{r,a}$:

$$G^{H_F}_{r,a} = G^{o}_{r,a} + G^{o}_{r,a}\, H_F\, G^{H_F}_{r,a} \qquad (2.18a)$$

where $G^{o}_{r,a}$ refers to retarded and advanced Green functions for the free electrons. Second, the description of the distribution of the particles in presence of collisions is given in terms of the field dependent Green functions. These functions satisfy the GKB basic equations:

$$G_{r,a} = G^{H_F}_{r,a} + G^{H_F}_{r,a} \Sigma_{r,a} G_{r,a} \qquad (2.18b)$$

$$\left[(G^{H_F})^{-1}, G^{>} \right] = \left[\Sigma, G^{>} \right] + \left[\Sigma^{>}, G \right] -$$

$$- \frac{1}{2} \left\{ \Sigma^{<}, G^{>} \right\} + \frac{1}{2} \left\{ \Sigma^{>}, G^{<} \right\} \qquad (2.18c)$$

To have a closed set of equations one needs to know the electron self energy Σ as a functional of the Green function G. To complete the notation let us remind that the following identities are valid for G (and Σ):

$$G(t,t') = \frac{1}{2} \left[G_a(t,t') + G_r(t,t') \right] \qquad (2.19a)$$

$$G_a(t,t') = \theta(t'-t)\left[G^<(t,t') - G^>(t,t')\right] \qquad (2.19b)$$

$$G_r(t,t') = \theta(t-t')\left[G^>(t,t') - G^<(t,t')\right] \qquad (2.19c)$$

$\theta(t-t')$ is the unit step function and $\{,\}$ indicates the anticommutator. Furthermore, as all G's are double time, double space, and real time Green functions, Eqs.(2.18) should be interpreted as matrix equations: integrals over intermediate position and time variables are implied throughout. In Eqs.(2.18c) all external forces are denoted by the operator H_F, whereas all scattering processes (impurities, phonons, etc..) are collected in the self energy. Eq.(2.19c) is a generalized quantum kinetic equation. The physical meaning of different terms is the following. The left hand side gives the collisionless evolution of the Green function. The right hand side represents a generalized collision integral: the commutators describe the kinetic effects of the interaction (renormalization of the electron eigenvalues due to the presence of field and interaction); the anticommutators describe the dynamical effects of the interaction (i.e. how

the collisions transfer particles from one energy-wavevector configuration to another). A consequence of the complete description of the interacting system is that the quasi-particle aproximation (i.e. a one to one correspondence between energy and wavevector) has to be relaxed. Now energy and wavevector are two independent variables described by a spectral density function $S(\vec{k},\epsilon)$ which gives the probability that the electron has the variables $(\vec{k},\epsilon)$.

As merits of this method: (i) The standard diagrammatic perturbation expansion for the interaction of the electrons with the scattering centers can be applied. Thus, collision broadening can be included from first principles. (ii) The intracollisional field effect is accounted for. (iii) Once $G^<$ is determined, the most interesting average quantities can be obtained straightforwardly.

As shortcomings: (i) To take advantage of the perturbation expansion an immaginary time domain has to be introduced. Therefore, an analytical continuation technique is necessary to obtain physical results on the real time domain.

2.6 The Wigner Representation

2.6.1 The Wigner Representation

The one-particle Wigner function $f_W(\vec{p},\vec{r};t)$ /2.22-24/ is defined as the Weyl transform of the density matrix $\rho(t)$ divided by h^3. In the case of a system in a pure state, f_W has the well known form given by Wigner:

$$f(\vec{p},\vec{r};t) = \frac{1}{h^3}\int d\vec{v}\ \psi^*(\vec{r}+\tfrac{1}{2}\vec{v},t)\ exp\left(\frac{i}{h}\vec{p}\cdot\vec{v}\right)\psi(\vec{r}-\tfrac{1}{2}\vec{v},t) \qquad (2.20)$$

where $\psi(r,t)$ is the wavefunction in configuration space. The average value of Eq.(2.2) becomes:

$$\langle O\rangle_t = \frac{1}{h^3}\iint o(\vec{p},\vec{r})\, f(\vec{p},\vec{r},t)\, d\vec{p}\, d\vec{r} \qquad (2.21)$$

where the function $o(\vec{p},\vec{r})$ is given by the Weyl correspondence rule:

$$o(\vec{p},\vec{r}) = \frac{1}{h^3}\,Tr\left\{O\iint d\vec{u}\, d\vec{v}\ exp\left[\frac{i}{h}\left((\vec{r}-\hat{q})\cdot\vec{u} + (\vec{p}-\hat{p})\cdot\vec{v}\right)\right]\right\} \qquad (2.22)$$

Circumflex accents disinguish the operator from the correspondent canonical variable.

The evolution equation of f_W is found by performing the Weyl transform of the Liouville von Neumann equation. A kinetic equation which includes collisional broadening and intracollisional field effects has been proposed in Ref./2.25/. Going over a second quantized formalism in the Heisenberg picture, the Wigner function is found to emerge from the Green function formalism. Indeed, by introducing Wigner coordinates:

$$\vec{r} = \vec{r}_1 - \vec{r}_1' \quad ; \quad t = t_1 - t_1'$$
$$\vec{R} = \frac{\vec{r}_1 + \vec{r}_1'}{2} \qquad T' = \frac{t_1 + t_1'}{2} \tag{2.23}$$

and defining Wigner transform:

$$G^<(\vec{R},\vec{P};\omega,T') = \int d\vec{r} \int_{-\infty}^{+\infty} dt \; exp\left[-i(\vec{P}\vec{r} - \omega t)\right] \times$$
$$\times (-i)\, G^<(\vec{R},\vec{r};t,T') \tag{2.24a}$$

$$G^{<}(\vec{R},\vec{r};t,T) = G^{<}(\vec{R}+\frac{\vec{r}}{2},T+\frac{t}{2};\vec{R}-\frac{\vec{r}}{2},T-\frac{t}{2}) \quad (2.24b)$$

it is:

$$f(\vec{P},\vec{R};T) = \frac{1}{(2\pi)}\int d\omega\, G^{<}(\vec{R},\vec{P};\omega,T) \quad (2.25)$$

Thus the kinetic equation (2.18) is appropriate for introducing all relevant quantum effects into $f(\vec{R},\vec{P},T)$. Following this procedure Barker and coworkers /2.26-28/ have analyzed collisionless (ballistic) transport for particles interacting with model potentials.

As merits of the Wigner representation: (i) One can take advantage of the correspondence rule to introduce concepts, like Wigner trajectories /2.29/, which visualize quantum effects in a classical framework.

As shortcomings: (i) The interpretation of the Wigner distribution should be made carefully as, by not being necessarily positive definite, it has not a probability meaning. In this respect a generalized Wigner distribution $f(\vec{R},\vec{P};\omega,T) = -i\ G^{<}(\vec{R},\vec{P};\omega,T)$, which allows for an autocorrelation function interpretation, should be more

conveniently introduced /2.17,30,31/. In doing so, the identity between the generalized Wigner function and the Green function formalisms is clearly evidenced.

(ii) The stationary Wigner functions may not be obtained from the transport equation, unless possible initial conditions are restricted /2.24,32/. Instead, they satisfy an eigenvalue equation reviewed in Ref./2.33/.

2.6.2 The Wigner Function For The One-Dimensional Potential Step

An interesting example of Wigner representation is the one for the stationary solution of the one dimensional potential step /2.29/:

$$V(q) = \begin{cases} 0 & q < 0 \\ V_0 & q \geq 0 \end{cases} \qquad (2.25a)$$

The eigenfunctions of a particle of energy $0 < \epsilon < V_0$ subject to the above potential step are:

$$\psi(q) = \begin{cases} 2A \exp(i\alpha/2) \cos(kq - \alpha/2) & q < 0 \\ 2A \exp(i\alpha/2) \cos(\alpha/2) \exp(-\gamma q) & q \geq 0 \end{cases} \qquad (2.25b)$$

where

$$\exp(i\alpha) = \frac{ik + \gamma}{ik - \gamma} \quad ; \quad k = \frac{1}{\hbar}\sqrt{2m\epsilon}$$

$$\gamma = \frac{1}{\hbar}\sqrt{2m(V_o - \epsilon)} \qquad (2.25c)$$

and A is an arbitrary normalization constant.

By assuming that the system is prepared in the state represented by Eq.(2.25b) at time t=0, the corresponding Wigner distribution can be obtained from Eq.(2.20) applied to the one dimensional case. The result is:

$$f(q,p,0) = \frac{4|A|^2}{\pi\hbar}\exp(-2\gamma q)\left\{\cos\frac{2pq}{\hbar}\,\frac{4\gamma k^2}{\left[\left(\frac{2p}{\hbar}+k\right)^2+\gamma^2\right]\left[\left(\frac{2p}{\hbar}-k\right)^2+\gamma^2\right]}+\right.$$

$$\left.+\sin\frac{2pq}{\hbar}\,\frac{k^2\left(k^2+\gamma^2-4\frac{p^2}{\hbar^2}\right)}{\left[\left(\frac{2p}{\hbar}+k\right)^2+\gamma^2\right]\left[\left(\frac{2p}{\hbar}-k\right)^2+\gamma^2\right]\frac{p}{\hbar}}\right\} \quad \text{if } q>0$$

(2.25d)

and

$$f(q,p,0) = \frac{4|A|^2}{\pi\hbar}\left\{\cos\left(\frac{2pq}{\hbar}-2kq\right)\frac{\gamma k}{\left[\gamma^2+\left(\frac{2p}{\hbar}-k\right)^2\right]\frac{2p}{\hbar}}-\right.$$

$$\left.-\cos\left(\frac{2pq}{\hbar}+2kq\right)\frac{\gamma k}{\left[\gamma^2+\left(\frac{2p}{\hbar}+k\right)^2\right]\frac{2p}{\hbar}}-\sin\left(\frac{2pq}{\hbar}-2kq\right)\times\right.$$

$$\times \frac{k\left(\frac{2P}{\hbar}k - k^2 + \gamma^2\right)}{\left[\gamma^2 + \left(\frac{2P}{\hbar} - k\right)^2\right]\frac{4P}{\hbar}\left(\frac{P}{\hbar} - k\right)} - \sin\left(\frac{2Pq}{\hbar} + 2kq\right) \times$$

$$\times \frac{k\left(\frac{2P}{\hbar} + k^2 - \gamma^2\right)}{\left[\gamma^2 + \left(\frac{2P}{\hbar} + k\right)^2\right]\frac{4P}{\hbar}\left(\frac{P}{\hbar} + k\right)} \Bigg\} \qquad \text{if } q < 0$$

(2.25e)

Since the particle is in an energy eigenstate, Wigner trajectories are given by equi-Wigner curves. Fig. 2.4 shows the results. The classical trajectories for the present case (see Fig.2.4(b)) consist simply of straight horizontal lines. An interesting feature exhibited by Wigner trajectories shown here (see Fig.2.4(c)) is that a non negligible portion of the trajectories penetrate through the potential step. In general, the larger the energy of the space-phase point approaching the potential step, the deeper is the penetration . Very roughly, the average penetration can be estimated by looking at the trajectories and their relative weights given by f. This approach thus provides a pictorial view of quantum tunnelling. One, however, should not attach a physical meaning to each single trajectory because it is not observable. As can be seen

from Fig.2.4(c) some trajectores are associated with negative weights. This is due to the fact that the Wigner distribution function is not positive definite. The Wigner distribution function is essentially an auxiliary mathematical function introduced for convenience of discussion. For the sake of completeness, Figs.2.5-7 report the full Wigner function in the classical phase space for the different particle energies there indicated.

2.7 Applications

Real cases can be classified within two limiting regimes of motion: the time reversible collisionless case and the irreversible stationary case when a given particle undergoes many completed collisions. The formal theories outlined in the previous section cannot be applied "sic et simpliciter" to the latter case. Indeed to identify a given number of completed collisions a coarse-graining of time is required. This problem concerns the reduction of the original non-Markovian generalized collision integral to a Markovian form. This procedure, which is at the basis of irreversibility, is however associated with a loss of information which is hard to evaluate in terms of physical approximations. This is the actual bottleneck of quantum transport theory.

Using the Green function method as a guide line, an interesting attempt to account for quantum effects within a standard Monte Carlo procedure has been proposed by Hess and coworkers /2.34-36/. A self-energy model for an electron nonpolar optical-phonon scattering mechanism is introduced as:

$$\Sigma(\epsilon) = g^2 \int d\epsilon' \frac{\rho_0(\epsilon')}{\epsilon - \epsilon' - \hbar\omega_{op} - \Sigma(\epsilon - \hbar\omega_{op}) + i\delta} \qquad (2.26)$$

where g is the coupling constant given by $\hbar D^2/(2\bar{\rho}\,\omega_{op})$ ($\hbar$ being the Planck constant divided by 2π, D is the optical phonon deformation constant, $\bar{\rho}$ the density of the material) and $\rho_0(\epsilon)$ the electron density of states.

Eq.(2.26) is solved numerically using a density of states obtained from pseudopotential calculations. The optical theorem allows to define the scattering rate for the electron phonon interaction as:

$$\tau^{-1}(\epsilon) = -\left(\frac{2}{\hbar}\right) Im\,\Sigma(\epsilon) \equiv -\left(\frac{2}{\hbar}\right)\Gamma \qquad (2.27)$$

which should, in principle, improve the Golden rule result. Indeed, self-energy corrections are found to reduce the scattering rate. Furthermore, the delta functions appearing in the energy conservation terms of the Golden rule are replaced by Lorentzian structures of the type:

$$\delta(\bar{\epsilon}_f - \bar{\epsilon}_i) \longrightarrow \frac{1}{\pi} \frac{(\Gamma_i + \Gamma_f)}{(\bar{\epsilon}_i - \bar{\epsilon}_f)^2 + (\Gamma_i + \Gamma_f)^2} \qquad (2.28)$$

where subscripts i and f indicate the initial and final

states, and $\bar{\epsilon}_{i,f}$ are the quasi-particle energies shifted by the real part of the self energy. Within a Monte Carlo procedure, Eq.(2.27) can be used for the determination of the free flight (self-energy correction) and Eq.(2.28) for the determination of initial and final states (collisional broadening). The latter step is a delicate one since it is not clear how it could be included consistently into numerical calculations. This point needs a more careful analysis than that presently available.

Several authors have recently speculated about the field dependence of the transition rates in high field quantum transport. Within a Stark ladder representation Sawaki /2.37/ has analyzed the effect of an electric field in terms of the self energy due to higher order terms in the elecron phonon interaction. Herbert and coworkers /2.38,39/ have used a time dependent perturbation theory modeling the scattering between Airy functions. Analogous calculations have been performed by Ziep and Keiper /2.40/. Marsh and Inkson /2.41/ have attempted to generalize the above results by employing WKB wavefunctions in place of Airy functions. Overall, no definite conclusions have been reached so far, and different approaches are still a matter of discussion /2.42/.

2.8 Conclusions

Recent developments on quantum transport in the hot-electron field has been surveyed. By comparing different formal approaches, the Green function method emerges as a more powerful technique since it can take advantage of a diagrammatic perturbation expansion for the interaction of carriers with the scattering centers. The comparison between theory and experiments /2.34, 35, 43-45/is still far from being satisfactory, in view of the difficulties to estimate the reliability of the approximations introduced and to find crucial experiments on the subject.

REFERENCES

2.1 J.R. Barker and D.K. Ferry, Sol. St. Electron. 23, 531 (1980).

2.2 K.K. Thornber, Sol. St. Electron. 21, 259 (1978).

2.3 J.R. Barker, Sol. St. Electron. 21, 267 (1978).

2.4 G.D. Mahan: Many Particle Physics (Plenum, New York, 1981).

2.5 Proc. 3rd Int. Conf. on Hot Electron, J. de Physique Colloque C7, Supplement 10, Tome 42 (1981).

2.6 C. Jacoboni and L. Reggiani, Rev. Mod. Phys. 55, 645 (1983).

2.7 S.Nakajima, Prog.Theor. Phys. 20, 948 (1958); R. Zwanzig, J. Chem. Phys. 33, 1338 (1960); R. Zwanzig, Physica 30, 1109 (1964).

2.8 N. Pottier and D. Calecki, Physica 110A, 471 (1982).

2.9 N. Pottier, Proc. 16th I.C.C.S., Physica 117B, 241 (1982).

2.10. N. Pottier, Physica 121A, 293 (1983).

2.11 H. Mori, Prog. Theor. Phys. 33,423 (1965).

2.12 D.N. Zubarev: Nonequilibrium Statistical Mechanics, Ed. P. Gray (Consultant bureau, London, 1974).

2.13 H. Grabert: Projection Operator Techniques in Nonequilibrium Statistical Mechaniscs, Vol. 95 (Springer Tracts in Modern Physics, Heidelberg, 1982).

2.14 J.J. Niez and D.K. Ferry, Phys. Rev. B28, 889 (1983).

2.15 J.J. Niez, K.S. Yi and D.K. Ferry, Phys. Rev. B28,

1988 (1983).

2.16 W. Poetz and D.K. Ferry, Proc. 17th I.C.P.S. Springer Verlag (New York,1985)p. 1329.

2.17 L.P. Kadanoff and G. Baym: Quantum Statistical Mechanics (Benjamin, New York, 1962).

2.18 D.C. Langreth and J.W. Wilkins, Phys. Rev. B6, 3189 (1972).

2.19 A.P. Jauho and J.W. Wilkins, Phys. Rev. Lett. 49, 762 (1982).

2.20 A.P. Jahuo and J.W. Wilkins, Phys. Rev. 29B, 1919 (1984).

2.21 For a review on the Green function formalism see: Chou Kuong-chao, Zhao-bin Su, Bai-lin Hao and Lu Yn, Phys. Repts. 118, 1 (1985).

2.22 E. Wigner, Phys. Rev. 40, 749 (1932).

2.23 F. Soto-Eguibar and P. Claverie, J. Math. Phys. 24, 1104 (1983).

2.24 M. Hillery, R.F. O'Connel, M.O. Scully and E.P. Wigner, Phys. Repts. 106, 121 (1984).

2.25 J. Lin and L.C. Chin, J. Appl. Phys. 57, 1373 (1985).

2.26 J.R. Barker and S. Murray, Phys. Lett. 93A, 271 (1983).

2.27 J.R. Barker, S. Collins, D. Lowe and S. Murray, Proc. 17th I.C.P.S. Springer Verlag ,New York (1985) p. 449.

2.28 J.R. Barker, Physica 134B, 22 (1985).

2.29 H.W. Lee and M.O. Scully, Found. Phys. 13, 61 (1983).

2.30 W. Hansch and G.D. Mahan, Phys. Rev. 28B,1902 (1983).

2.31 G.D. Mahan, Phys. Repts. 110, 321 (1984).

2.32 V.I. Tatarskii, Sov. Phys. Usp. 26, 311 (1983).

2.33 P. Carruthers and F. Zachariasen, Rev. Mod. Phys. 55, 245 (1983).

2.34 Yia-Chung Chang, D.Z.Y. Ting, J.Y. Tang and K. Hess, Appl. Phys. Lett. 42, 76 (1983).

2.35 J.Y. Tang and K. Hess, J. Appl. Phys. 54, 5139 (1983); ibidem 5145 (1983).

2.36 K. Hess and G.J. Iafrate, Hot electrons in semiconductor heterostructures and superlattices, in: Hot-Electron Transport in Semiconductors, Topics in Applied Physics Vol. 58, Ed. L. Reggiani (Springer Verlag, Heidelbergh, 1985) pp. 200-227.

2.37 N. Sawaki, J. Phys. C16, 4611 (1983).

2.38 D.C. Herbert and J.J. Till, J. Phys. C15, 5411 (1982); ibidem C16, 49 (1983).

2.39 D.C. Herbert, J. Phys. C17, 6749 (1984).

2.40 O. Ziep and R. Keiper, Phys. Stat. Sol. 128b, 779 (1985).

2.41 A. Marsh and J.C. Inkson, J. Phys. C17, 4601 (1984).

2.42 D. Lowe, J. Phys. C18, 2209 (1985).

2.43 K. Brennan and K. Hess, Solid State Electron. 27, 347 (1984).

2.44 W. Porod and D.K. Ferry, Physica 134B, 137 (1985).

2.45 S.D. Brorson, D.J. Di Maria, M.V. Fischetti, F.L. Pesavento, P.M. Solomon
and D.W. Dong, J. Appl. Phys 58, 1302 (1985).

TABLE CAPTIONS

Table 2.1: Theoretical levels of description in nonequilibrium statistical mechanics.

Table 2.2: The most interesting phenomena predicted by quantum transport theory.

LIOUVILLE VON NEUMANN EQUATION

↓

KINETIC QUANTUM TRANSPORT

i) Generalized Master Equation

ii) Generalized Langevin Equation

iii) Green Function Method

iv) Wigner Distribution

↓

SEMICLASSICAL BOLTZMANN EQUATION

i) Band structure: the energy is given by a well definite function of $\vec{k}$

ii) Scattering Probability: within the golden rule

iii) Classical concept of the single particle distribution function as the probability of finding the particle in $d\vec{k}$ about $\vec{k}$ and $d\vec{r}$ about $\vec{r}$

TAB. 2.1

NEW PHENOMENA

INTRA COLLISIONAL FIELD EFFECT

THE SCATTERING EVENT DURING A FINITE TIME, AND THE APPLIED ELECTRIC FIELD INTERFERES WITH THE SCATTERING HAMILTONIAN

COLLISIONAL BROADENING

OWING TO SCATTERING PROCESSES THE ELECTRON STATE HAS A FINITE LIFETIME. THEREFORE THE ENERGY WAVEVECTOR RELATIONSHIP IS DESCRIBED BY A SPECTRAL DENSITY $S(\vec{k}, \epsilon)$. $S(\vec{k}, \epsilon)$ IS THE PROBABILITY OF FINDING THE ELECTRON WITH GIVEN $(\vec{k}, \epsilon)$.

CONSEQUENCE

SHARP PEAKS OCCURRING AT THRESHOLD ENERGIES ARE SMOOTHED

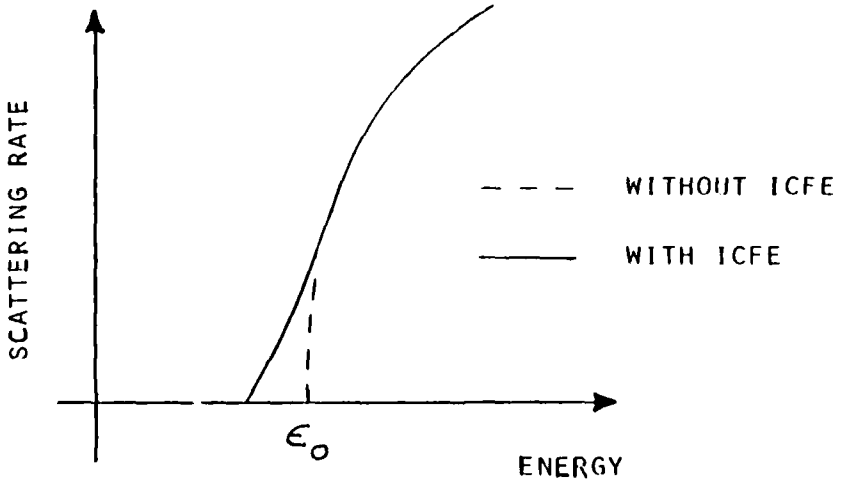

TAB. 2.2

FIGURE CAPTIONS

Fig. 2.1: Schematic representation of the semiclassical Boltzmann picture.

Fig. 2.2: Schematic representation of the Intra-Collision Field Effect.

Fig. 2.3: Schematic representation of Collision Broadening.

Fig. 2.4: Representation of the Wigner trajectories for the one-dimension potential step model (arbitrary units are used).

(a) Profile of the potential.

(b) Classical trajectory for the case of a particle energy $\in$ lower than the potential energy of the barrier V_0.

(c) Wigner trajectories for the case $\in = 0.5$, $V_0 = 1$.

Fig. 2.5: Plot of the Wigner function for the one dimension potential step model in phase-space. $\in = 0.1$; $V_0 = 1$ in arbitrary units.

Fig. 2.6: The same as in Fig. 2.5 for $\epsilon = 0.5$; $V_o = 1$.

Fig. 2.7: The same as in Fig. 2.5 for $\epsilon = 0.99$; $V_o = 1$.

SEMICLASSICAL BOLTZMANN PICTURE

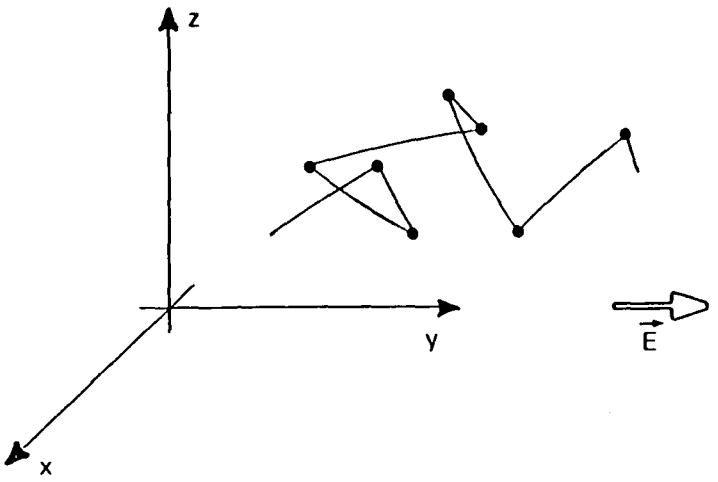

CLASSICAL TRAJECTORIES

POINT LIKE COLLISIONS

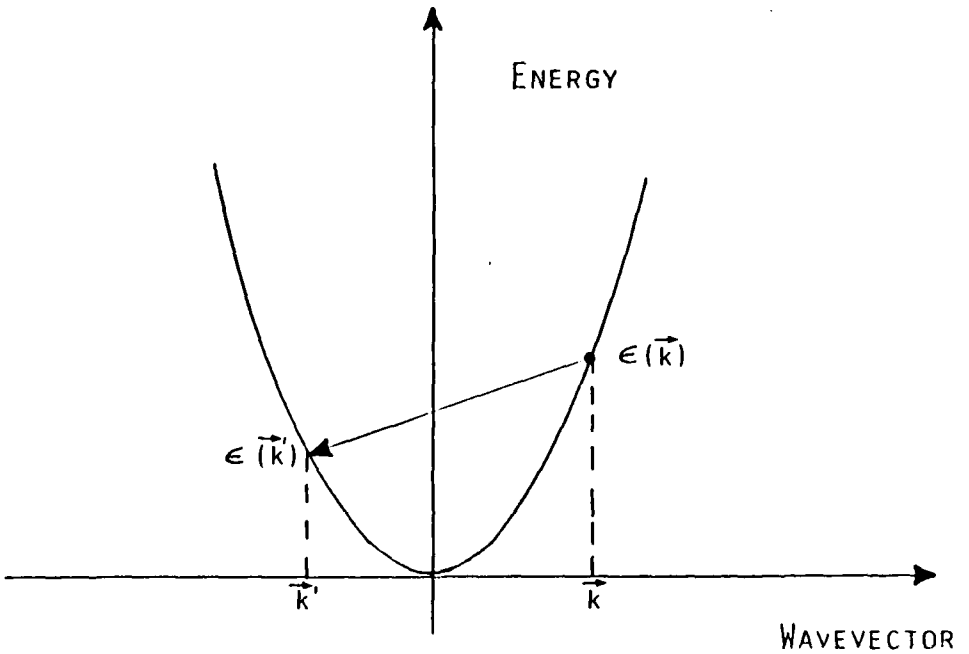

$$P(\vec{k},\vec{k}') \propto \delta(\epsilon(\vec{k}) - \epsilon(\vec{k}') \pm \hbar\omega_q)$$

FIG. 2.1

INTRA COLLISIONAL FIELD EFFECT

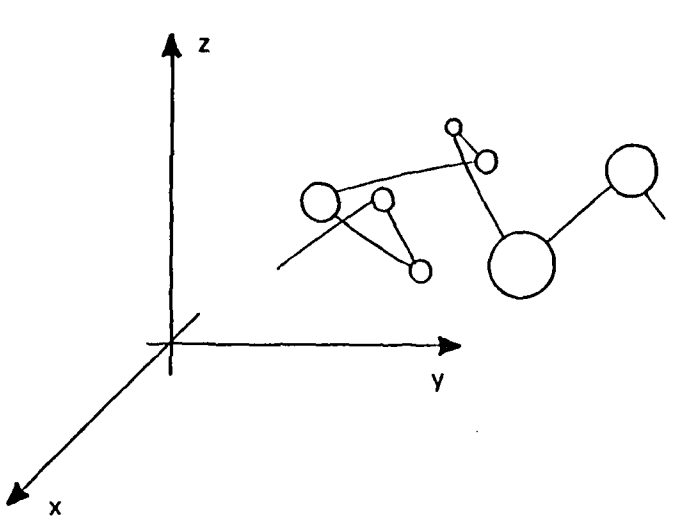

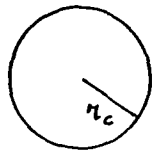

COLLISION SPHERE

$$\begin{cases} r_c \approx \dfrac{\hbar q}{m} \tau_c \\ r_c \approx \left[\dfrac{2m}{\pi \, |e\vec{q}\cdot\vec{E}|} \right]^{1/2} \end{cases}$$

ENERGY CAN BE GAINED OR LOST FROM THE FIELD DURING THE COLLISION

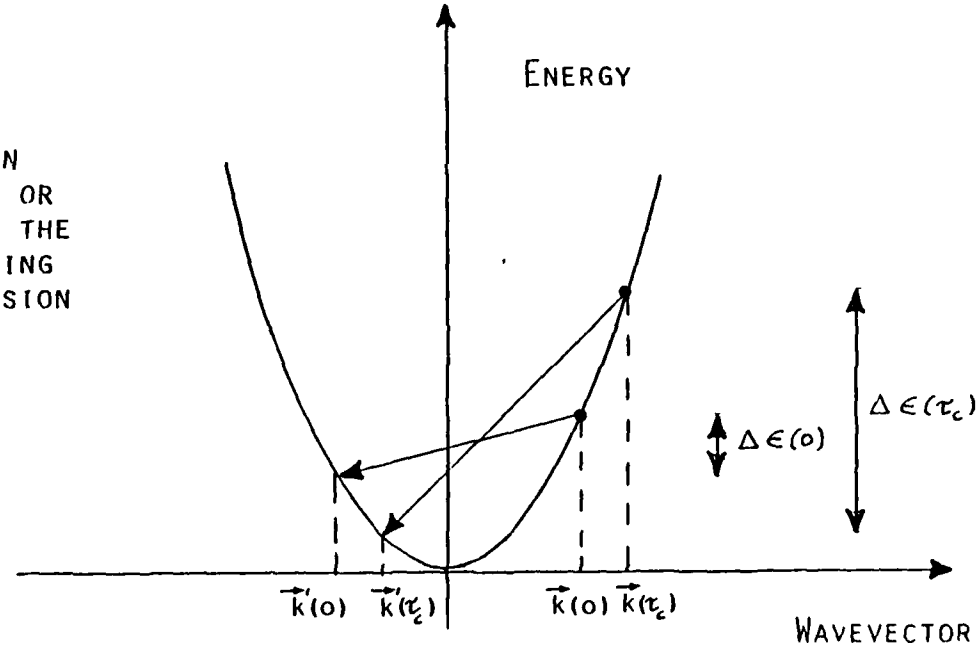

$$P(k,k') \propto \int_0^\infty dt \cos\left\{ \frac{t}{\hbar} \left[\epsilon(\vec{k}) - \epsilon(\vec{k}') \pm \hbar\omega_q - \frac{e\hbar\vec{E}\cdot\vec{q}\,t}{2m} \right] \right\}$$

FIG. 2.2

COLLISIONAL BROADENING

QUASI-PARTICLE SELF-ENERGY $\Sigma(\vec{k},\epsilon)$

$$\epsilon = \epsilon_{\text{kinetic}}(\vec{k}) + \text{Re}\{\Sigma(\vec{k},\epsilon)\}$$

$$\tau = \left[-\frac{2}{\hbar}\ \text{Im}\{\Sigma(\vec{k},\epsilon)\}\right]^{-1}$$

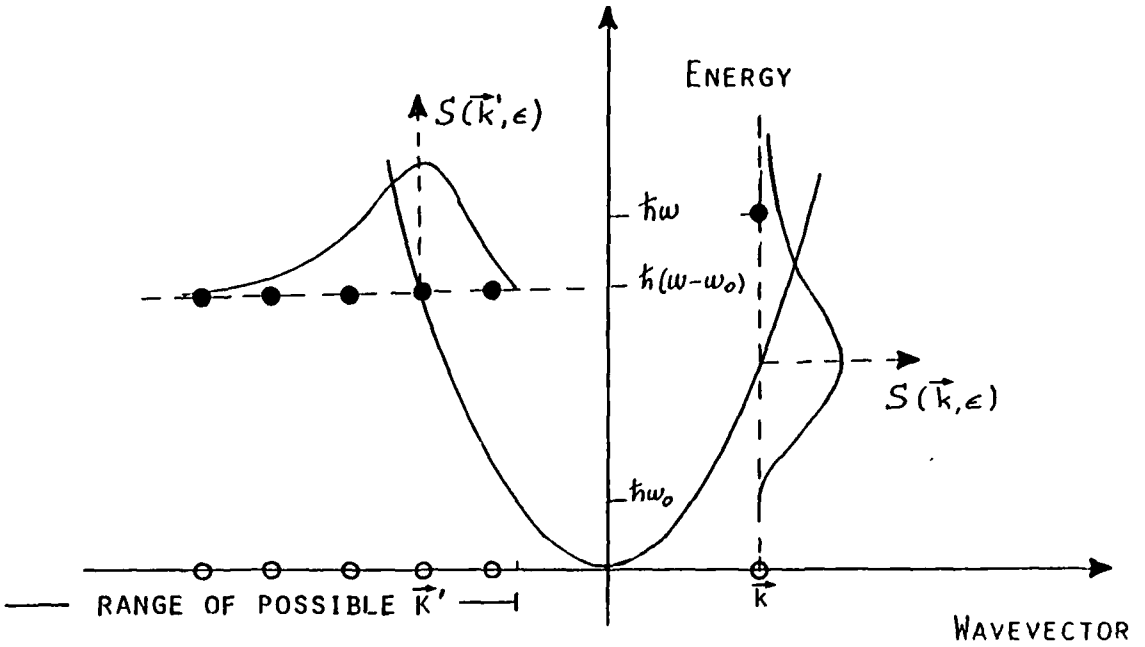

$$P(\vec{k},\vec{k}') \propto \frac{\text{Im}\{\bar{\Sigma}\}}{\left[\bar{\epsilon}-\bar{\epsilon}_{\text{kinetic}}-\text{Re}\{\bar{\Sigma}\}\right]^2+\left[\text{Im}\{\bar{\Sigma}\}\right]^2}$$

FIG. 2.3

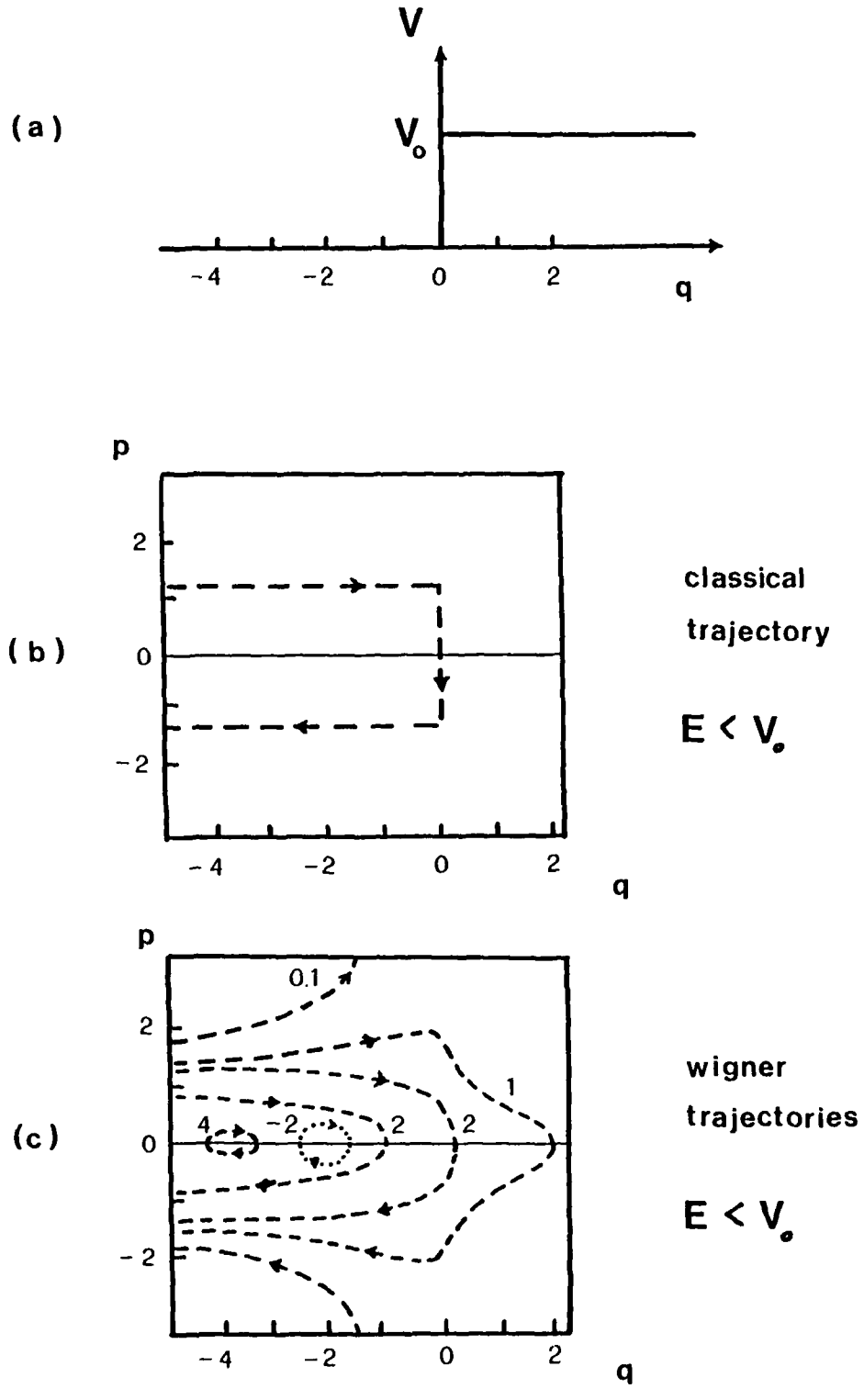
(a)
V
V_o
-4
-2
0
2
q
(b)
p
2
0
-2
-4
-2
0
2
q
classical
trajectory
$E < V_o$
(c)
p
0.1
1
4
-2
2
2
2
0
-2
-4
-2
0
2
q
wigner
trajectories
$E < V_o$

FIG. 2.4

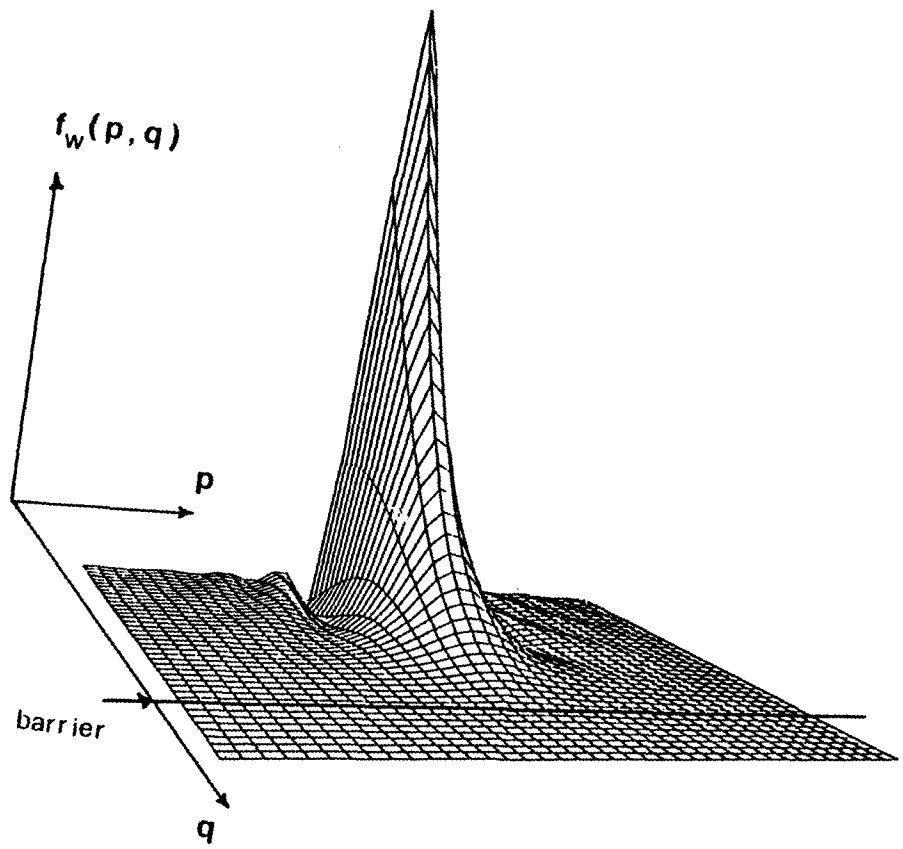

FIG. 2.5

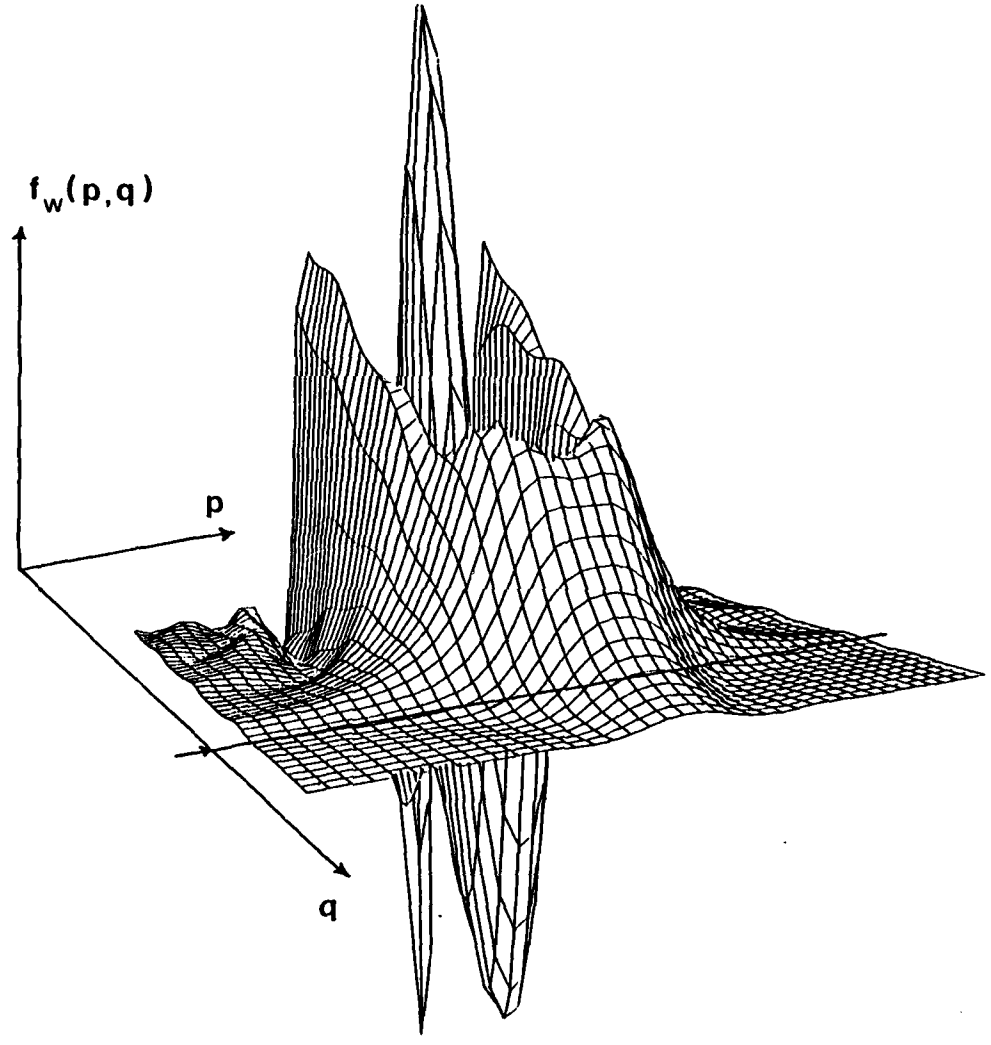

FIG. 2.6

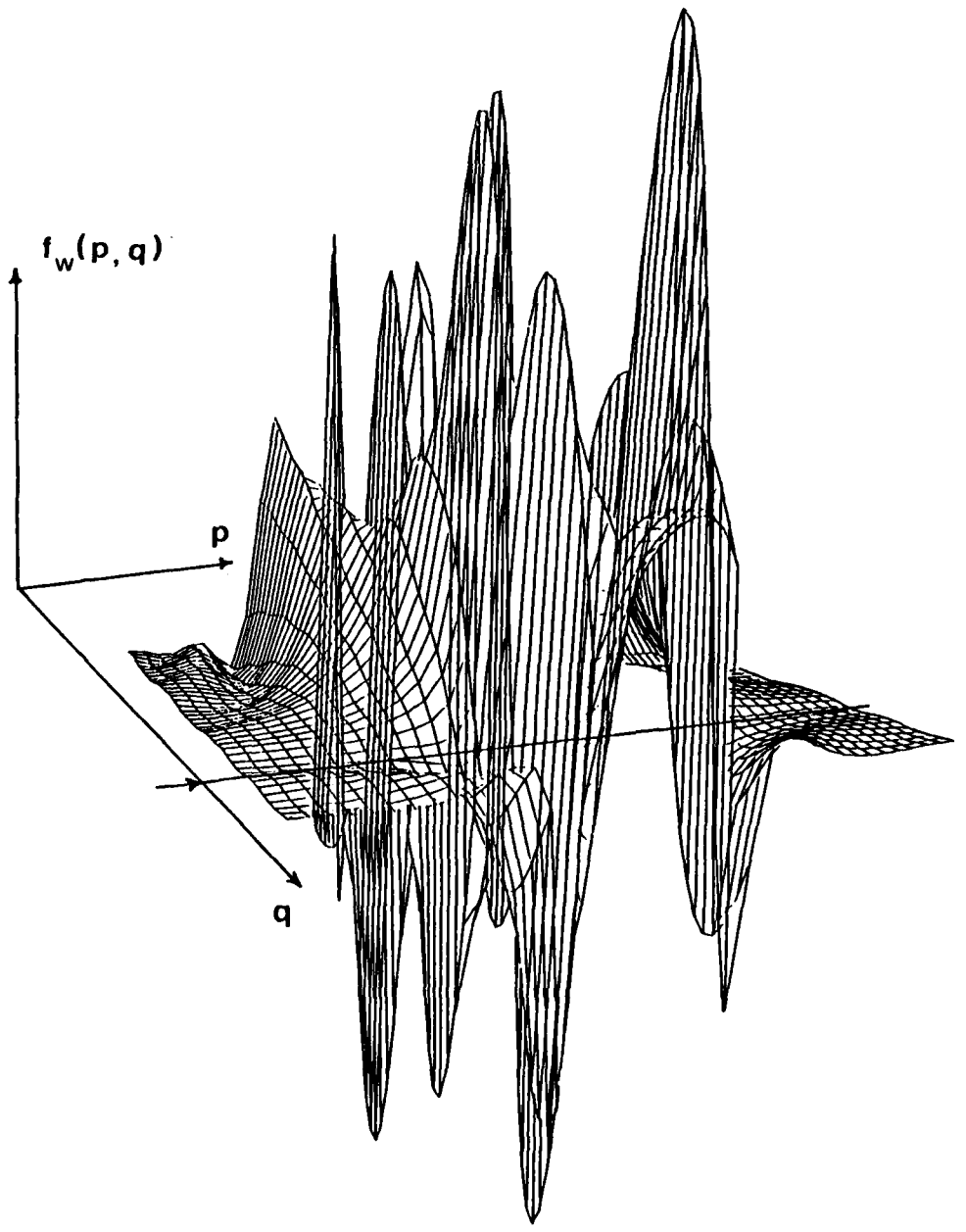

FIG. 2.7

3. MONTE CARLO SOLUTIONS OF TRANSPORT-LIKE EQUATIONS

3.1 Assumptions and limits of the traditional Monte Carlo procedure

The Monte Carlo method, as applied to charge transport in semiconductors, consists of a simulation of the motion of one or more electrons inside a crystal, subject to the action of external forces due to applied electric and magnetic fields and of given scattering mechanisms. The duration of the carrier free flight (i.e., the time between two successive collisions) and the scattering events involved in the simulation are selected stochastically in accordance with some given probabilities describing the microscopic processes.

As a consequence, any Monte Carlo method relies on the generation of a sequence of random numbers with given probability distribution.

When the purpose of the analysis is the investigation of a steady-state homogeneous phenomenon, it is sufficient in general to simulate the motion of one single electron: from ergodicity we may assume that a sufficiently long path of this sample electron will give information on the behavior

of the entire electron gas. When, on the contrary, the transport process under investigation is not homogeneous or is not stationary, then it is necessary to simulate a large number of electrons (Ensemble Monte Carlo) and follow them in their dynamic histories in order to obtain the desired information on the process of interest.

The electron distribution function can be obtained from a Monte Carlo simulation by extracting the information on how much time the simulated particle spends in each cell of a mesh of the phase-space or, in an Ensemble Monte Carlo, by counting the number of particles in each cell of the mesh.

It is well known that the distribution function obtained from a Monte Carlo simulation is a solution of the Boltzmann equation describing the same physical situation. However, the power of the method goes beyond this characteristics. In fact, since the scattering events are explicitely simulated according to the scattering cross sections of the model, fluctuations actually arise in the simulated process and quantities like autocorrelation functions and noise can be studied/3.1/.

Such a situation is so favorable for the analysis of transport problems that, in the last two decades, most of

the physical systems of interest have been analysed and understood within the limits of validity of the semiclassical theory of transport.

Therefore, a need is now felt to overcome these limits and try to extend the method of Monte Carlo simulation to include quantum effects not accounted for in the traditional approach.

Such a need is further justified, on practical grounds, by the present state of VLSI technology which now allows the fabrication of devices so small that quantum effects may become appreciable.

Quantum effects are a consequence of small dimensions not only because of the well known size effects, but also because the applied voltages (which cannot be decreased below certain limits) at such distances imply very high fields, at which quantum phenomena may become important

In the traditional semiclassical approach, collisions are treated as pointlike events in both space and time. In fact, a fully quantum mechanical treatment should account for the interference between applied and scattering fields (intracollisional field effects), the finite lifetime of the electron states (collisional broadening), and the

possibility of multiple collisions.

Within this picture, energy conservation is not a feature of each of each scattering event, and the simple one to one correspondence between energy and wavevector will be substituted by a probability distribution $P_k(\epsilon)$. Furthermore, at any new collision the assumption is made of perfect energy conservation of the previous collision, which is not exact when two scattering events happen quite near to each other. Collision broadening is thus neglected.

Another feature of the traditional approach which we do not feel happy about is the use of first order perturbation theory, that is the use of the Fermi golden rule, for the transition probabilities.

The situation then calls for a search of new techniques which can allow us to treat transport problems with a fully quantum approach, free from the above limitations.

3.2 Monte Carlo solution of a set of algebric equations

Let us consider a system of n linear algebric equations of the type

$$x_i = f_i + A_{ij}\, x_j \,, \quad ij = 1,2,\ldots n \qquad (3.1)$$

where x_i are the unknowns, f_i a known set of numbers and A_{ij} a matrix of known coefficients, and summation over repeated indices is implied.

If Eq.(3.1) is iteratively substituted into itself, we obtain the following expansion in series of A:

$$x_i = f_i + A_{ij}\,(f_j + A_{jk}\, x_k) \qquad (3.2)$$

$$= f_i + A_{ij}\, f_j + A_{ij}\, A_{jk}\, f_k + \ldots + A_{ij}\, A_{jk} \ldots A_{lm}\, f_m + \cdots$$

If

$$\max_i \sum_{j=1}^{n} | A_{ij} | < 1 \qquad (3.3)$$

the series in Eq.(3.2) converges/3.2/.

It may be interesting to put Eq.(3.2) in the form

$$(I-A)x = f \tag{3.4}$$

or

$$x = (I-A)^{-1} f \tag{3.5}$$

In this way we recognize the series expansion in Eq.(3.2) as the harmonic series expansion of the resolvant operator in Eq.(3.5):

$$(I-A)^{-1} = 1+A+A^2+... \tag{3.6}$$

A Monte Carlo procedure has been developed by Von Neumann and Ulam to solve the system in Eq.(3.1), which proceeds as follows/3.2/.

Let us consider a set of n "states" or "boxes" labelled 1, 2, ...n, and let a "simulative particle" be positioned at the beginning of the simulation in box i. Let then simulate a terminating random walk with fixed but arbitrary

transition probabilities

$$p_{ij} \quad , \quad i,j=1,\ldots n \tag{3.7}$$

from state i to state j. p_{ij} must satisfy the following conditions:

$$p_{ij} \geq 0 \qquad (>0 \text{ if } A_{ij} \neq 0)$$

$$\sum_{j}^{1} p_{ij} < 1 \qquad i=1,\ldots n \tag{3.8}$$

For each state i the random walk has a terminating probability given by

$$p_{i} = 1 - \sum_{j}^{1} p_{ij} \tag{3.9}$$

Any random walk γ may be represented by the set of the successive visited states

$$\gamma = (i_0, i_1, \ldots, i_{k-1}, i_k) \tag{3.10}$$

For a given random walk represented by γ in Eq.(3.10) let us compute the quantity

$$X(\gamma) = V(\gamma) \cdot \frac{f_{ik}}{p_{ik}} \tag{3.11}$$

where

$$V(\gamma) = \frac{A_{i_0 i_1}}{p_{i_0 i_1}} \cdot \frac{A_{i_1 i_2}}{p_{i_1 i_2}} \cdots \frac{A_{i_{k-1} i_k}}{p_{i_{k-1} i_k}} \tag{3.12}$$

or

$$V(\gamma)=1 \quad \text{if} \quad \gamma=(i_0) \tag{3.13}$$

The expression $\gamma=(i_0)$ in the last equation means that the random walk has terminated before any transition took place. The expectation value of $X(\gamma)$ for random walks starting from i_0 is given by

$$X(\gamma/i_0) = \sum_{\gamma/i_0} P(\gamma/i_0) X(\gamma/i_0) \tag{3.14}$$

where $P(\gamma/i_0)$ is the probability of having the random walk γ, given i_0 as starting state. Thus

$$\langle X(\delta/i_0)\rangle = \sum_{k=0}^{\infty} \sum_{i_1} \cdots \sum_{i_k} P(\delta/i_0) V(\delta) \frac{f_{i_k}}{p_{i_k}} =$$

$$= \sum_{k=0}^{\infty} \sum_{i_1} \cdots \sum_{i_k} p_{i_0 i_1} p_{i_1 i_2} \cdots p_{i_{k-1} i_k} \cdot$$

$$\cdot V(\delta) \cdot \frac{f_{i_k}}{p_{i_k}} =$$

$$= \sum_{k=0}^{N} \sum_{i_1} \cdots \sum_{i_k} p_{i_0 i_1} p_{i_1 i_2} \cdots p_{i_{k-1} i_k} \cdot$$

$$\cdot \frac{A_{i_0 i_1}}{p_{i_0 i_1}} \cdots \frac{A_{i_{k-1} i_k}}{p_{i_{k-1} i_k}} \cdot f_{i_k} =$$

$$= f_{i_0} + \sum_{i_1} A_{i_0 i_1} f_{i_1} + \sum_{i_1 i_2} A_{i_0 i_1} A_{i_1 i_2} f_{i_2} + \cdots$$

$$= f + Af + A^2 f + \cdots = X_{i_0}$$

where we have taken into account Eq.(3.2).

Therefore the following Monte Carlo procedure can be applied in order to solve the system in Eq.(3.1): a given unknown x_0 is chosen and many random walks are performed starting from

the state i_0 , according to the transition and terminating probabilities given in Eqs.(3.7-9). For each random walk, the quantity $X(\gamma)$ in Eq.(3.11) is evaluated. Its average value over the random walks is a correct estimator for x_0. Variations of this method can be found in the literature/3.2/.

3.3 Generalization of the procedure to an integro-differential equation

Let us consider an integro-differential equation of the type

$$\frac{\partial f(x,t)}{\partial t} = -v\frac{\partial f(x,t)}{\partial x} + \int_a^b H(x,x',t)f(x',t)dx' \qquad (3.16)$$

where v is a constant and H(x,x',t) is a known function; f(x,t) is the unknown function defined in the interval $a \leq x \leq b$.

The interest in considering this equation is based on the fact that transport equations have often this form. In particular the Boltzman Equation can be reduced to the form of Eq.(3.16) with H closely related to the scattering probabilities and v proportional to the applied electric field.

In what follows we shall describe a numerical procedure which generalizes the method shown in the previous section to find a steady state solution, if it exists, of an equation of the type of Eq.(3.16).

From Eq.(3.16) we may obtain

$$f(x,t+\delta t) - f(x,t) = v\delta t \frac{\partial f(x,t)}{\partial x} + \int_a^b H(x,x',t)\delta t f(x',t)dx' \qquad (3.17)$$

or

$$f(x,t+\delta t) = f(x-\delta x,t) + \int_a^b H(x,x',t)\delta t f(x',t)dx' \qquad (3.18)$$

where $x=v\delta t$.

Let us consider a mesh of the interval (a,b) and let $f_i(t)$ be the value of f(x,t) in a representative value of x in the i-th interval. If x is in cell i, let $x-\delta x$ be in cell i'. Then our equation reduces to

$$f_i(t+\delta t) = f_{i'}(t)+A_{ij} f_j(t) \qquad (3.19)$$

where

$$A_{ij} = \int_{cell\ j} H(x_i, x', t)\, \delta t\, dx' \qquad (3.20)$$

If Eq.(3.16) has an asymptotic solution independent of t, for large enough t Eq.(3.19) reduces to

$$f_i = f_{i'} + A_{ij} f_j \qquad (3.21)$$

This equation is not exactly of the type desired (Eq.(3.21)) since $f_{i'}$ is not known. However an iterative procedure can be attempted which starts with a trial function $f^{(0)}$; If $f^{(0)}$ is inserted in the first term of the r.h.s. of Eq.(3.21), then with the Monte Carlo procedure indicated above a solution $f^{(1)}$ can be found, solution of the equation

$$f_i^{(1)} = f_{i'}^{(0)} + A_{ij}^{(1)} \qquad (3.22)$$

The process can be repeated with $f^{(1)}$ as known term, to find the next iteration $f^{(2)}$, and so on until convergence is

reached.

We have tested the above procedure for the case of

$$H(x,x',t) = \sqrt{\frac{2}{\pi}} \frac{e^{-(x^2-x'^2)} \left(e^{-t}(2x^2v - x - v) + 2x \cdot v\right)}{(x'e^{-t} + 1)} \qquad (3.23)$$

where x is variable in the whole real axis. In this case the equation has the solution, nomalized to unity,

$$f(x,t) = \sqrt{\frac{1}{\pi}}\, e^{-x^2} \left(x e^{-t} + 1\right) \qquad (3.24)$$

with asymptotic solution given by

$$f(x,t) = \sqrt{\frac{1}{\pi}}\, e^{-x^2} \qquad (3.25)$$

The Monte Carlo procedure described above has been applied and the results are reported in Fig.3.1. Here the initial trial functionand the function obtained after a large number of random walks are shown together with the exact solution of the equation.

3.4 Application to a quantum transport equation

Let us consider an ensemble of N electrons in a crystal in the presence of a homogeneous static electric field E and a perturbation potential given by a superposition of plane waves with different wave vectors and equal frequency.

$$V(x,t) = \sum_q \left\{ A_q e^{i(qx-\omega_0 t)} + A_q^* e^{-i(qx-\omega_0 t)} \right\} \qquad (3.26)$$

This potential may be considered a semiclassical representation of an optical phonon field.

In what follows we shall adopt a density matrix formalism. The one-electron wave functions can be expanded in a series of Bloch states as

$$\Psi^{(i)}(\vec{r},t) = \sum_k C^{(i)}(k,t)\, u_k(\vec{r})\, e^{i\vec{k}\cdot\vec{r}} \qquad (3.27)$$

where i indicates the i-th electron.

The density matrix ρ is defined as

$$\rho(k,k',t) = \frac{1}{N}\sum_{i=1}^{N} C^{(i)}(k,t)\, C^{(i)*}(k',t). \qquad (3.28)$$

ρ can now be considered as an operator whose matrix elements in the base of the Bloch states are given by Eq.(3.28). The equation of motion for ρ is

$$i\hbar \frac{\partial \rho}{\partial t} = [H, \rho] \qquad (3.29)$$

In the base of Bloch states this equation becomes

$$i\hbar \frac{\partial \rho(k,k',t)}{\partial t} = \sum_{k''} \Big\{ H(k,k'',t)\rho(k'',k',t) - \rho(k,k'',t) \cdot H(k'',k',t) \Big\} \qquad (3.30)$$

If we include the time dependence in the basis set of functions, we may write, in this new interaction representation

$$\Psi^{(i)}(\vec{r},t) = \sum_k b^{(i)}(k,t)\, M_k(\vec{r})\, e^{i(k\vec{r}-\omega_k t)} \qquad (3.31)$$

with

$$b^{(i)}(k,t) = c^{(i)}(k,t)\, e^{i\omega_k t} \qquad (3.32)$$

The density matrix is now written as

$$a(k,k',t) = \frac{1}{N}\sum_{i=1}^{N} b^{(i)}(k,t)\, b^{(i)*}(k',t) = \rho(k,k',t)\, e^{i(\omega_k-\omega_{k'})t} \qquad (3.33)$$

By substituting ρ as given by this expression in Eq.(3.30) we obtain

$$i\hbar\frac{\partial}{\partial t}\left(a(k,k',t)\, e^{-i(\omega_k-\omega_{k'})t}\right) =$$

$$\sum_{k''} \Big\{ H(kk''t)\, a(k'',k',t) \cdot e^{-i(\omega_k-\omega_{k'})t} - a(kk't) \cdot e^{-i(\omega_k-\omega_{k''})t} H(k''k't) \Big\} \tag{3.34}$$

where

$$H(kk't) = \int d\vec{r}\, u_k^*(\vec{r})\, e^{i\vec{k}\cdot\vec{r}}\, H\, u_{k'} e^{ik'r} =$$

$$= \Big(\int d\vec{r}\, u_k^*(\vec{r})\, e^{-i\vec{k}\vec{r}}\, e^{i\omega_k t}\, H\, u_{k'}(\vec{r})\, e^{i\vec{k}'\vec{r}}\, e^{-i\omega_{k'}t} \Big) \cdot \tag{3.35}$$

$$\cdot e^{-i(\omega_k-\omega_{k'})t} = \mathcal{H}_b(kk't)\, e^{-i(\omega_k-\omega_{k'})t}$$

Now $\mathcal{H}_b(k,k',t)$ are the matrix elements of H between the time dependent Bloch states. For simplicity these will be approximated, in what follows, by plane waves, thus neglecting the overlap integrals in the matrix elements.

By inserting Eq.(3.35) into Eq.(3.34), we have

$$i\hbar \left(\frac{\partial a(kk't)}{\partial t} \right) e^{-i(\omega_k-\omega_{k'})t} + \hbar(\omega_k-\omega_{k'})\, a(kk't)\, e^{-i(\omega_k-\omega_{k'})t} =$$

$$= \sum_{k''} \left\{ \mathcal{H}_1(kk''t)\, e^{-i(\omega_k - \omega_{k''})t} \cdot a(k''k't)\, e^{-i(\omega_{k''} - \omega_{k'})t} \right. \tag{3.36}$$
$$\left. - a(kk''t)\, e^{-i(\omega_k - \omega_{k''})t}\, \mathcal{H}_1(k''k't)\, e^{-i(\omega_{k''} - \omega_{k'})t} \right\} \tag{3.36}$$

or

$$i\hbar \frac{\partial a(kk't)}{\partial t} + \hbar(\omega_k - \omega_{k'})\, a(kk't) = \sum_{k''} \left\{ \mathcal{H}_1(kk''t)\, a(k''k't) \right. \tag{3.37}$$
$$\left. - a(kk''t)\, \mathcal{H}_1(k''k't) \right\}$$

The total hamiltonian is given by the sum of three terms:

$\mathcal{H}_0$ = unperturbed hamiltonian for an electron in the perfect crystal;

$\mathcal{H}_E$ = hamiltonian due to the presence of the external field, here assumed uniform and constant;

$\mathcal{H}_S$ = hamiltonian due to the interaction with the oscillating (phonon) field given by Eq.(3.26).

For the matrix elements we have

$$\mathcal{H}_0(kk't) = e^{i(\omega_k - \omega_{k'})t} \in(k')\,\delta(k-k') \tag{3.38}$$

$$\mathcal{H}_E(kk't) = \frac{1}{2\pi}\int e^{-i(\vec{k}\vec{r}-\omega_k t)}\, e^{i(\vec{k}'\vec{r}-\omega_{k'}t)}\, eEx\, d\vec{r} =$$

$$= e^{i(\omega_k-\omega_{k'})t}\, eE\, i\frac{d}{dk}\,\frac{1}{2\pi}\int e^{-i(k-k')\hat{r}}\, d\hat{r} =$$

$$= e^{i(\omega_k-\omega_{k'})t}\, eE\, i\,\delta'(k-k') \tag{3.39}$$

$$\mathcal{H}_S(kk't) = \int \frac{1}{2\pi} e^{-i(\vec{k}\hat{r}-\omega_k t)}\, e^{i(\vec{k}'\hat{r}-\omega_{k'}t)} \cdot \left(\sum_q A_q e^{i(qx-\omega_0 t)} + c.c.\right) =$$

$$= \sum_q \left\{ A_q e^{i(\omega_k-\omega_{k'}-\omega_0)t}\,\frac{1}{2\pi}\int e^{-i(\vec{k}-\vec{k}'+\vec{q})\hat{r}}\, d\hat{r} + A_q^{*} e^{i(\omega_k-\omega_{k'}+\omega_0)t}\cdot\right.$$

$$\left.\cdot\,\frac{1}{2\pi}\int e^{-i(\vec{k}-\vec{k}'-\vec{q})\cdot\hat{r}}\, d\hat{r}\right\} =$$

$$= \sum_q A_q e^{i(\omega_k-\omega_{k'}-\omega_0)t}\,\delta(k-k'+q) + \sum_q A_q^{*} e^{i(\omega_k-\omega_{k'}+\omega_0)t}\cdot\delta(k-k'+q) =$$

$$= A_{k'-k}\, e^{i(\omega_k-\omega_{k'}-\omega_0)t} + A_{k'-k}\, e^{i(\omega_k-\omega_{k'}+\omega_0)t} \tag{3.40}$$

In order to consider V as representative of the phonon field

we choose

$$A_q = \sqrt{\frac{\hbar}{2\omega_0 \rho V}}\, E_1\, i\,|\vec{q}|\sqrt{N_q} \tag{3.41}$$

where ρ is the density of the crystal, V its volume, E_1 the deformation potential coupling constant, and N_q the phonon occupation number.

Furthermore, in the second term, corresponding to the emission of phonons N_q must be substituted by $N_q + 1$, in order to take into account spontaneous emission. Therefore

$$\mathcal{H}_S(kk't) = \sqrt{\frac{\hbar}{2\omega_0 \rho V}}\, E_1\, i\,|\Delta k|\left\{\sqrt{N_q}\, e^{-i(\omega_{k'}-\omega_k+\omega_0)t} - \sqrt{N_q+1}\, e^{-i(\omega_{k'}-\omega_k-\omega_0)t}\right\} \tag{3.42}$$

By substituting the matrix elements calculated above into Eq.(3.37) for the dynamics of the density matrics, we obtain

$$\frac{\partial a(kk't)}{\partial t} = -\dot{k}\left(\nabla_k + \nabla_{k'}\right) a(kk't) - i\dot{k}\left(\vec{v}_{k'} - \vec{v}_k\right) t\; a(kk't)$$

$$+\sum_{k''}\frac{E_1|\Delta k|}{\sqrt{2\hbar\omega_{\Delta k}\varepsilon V}}\left\{\left(\sqrt{N_q}\,e^{-i(\omega_{k''}-\omega_k+\omega_{\Delta k})t}-\sqrt{N_q+1}\,e^{-i(\omega_{k''}-\omega_k-\omega_{\Delta k})}\right)\right.$$

$$\cdot a(k''k't)-\left(\sqrt{N_q}\,e^{-i(\omega_{k'}-\omega_{k''}+\omega_{\Delta k})t}-\sqrt{N_q+1}\,e^{-i(\omega_{k'}-\omega_{k''}-\omega_{\Delta k})t}\right)$$

$$\left.\cdot a(kk''t)\right\} \qquad (3.43)$$

where $\vec{k} = eE/\hbar$ and $\vec{v}_k = \nabla_{\vec{k}}\omega_{\vec{k}}$.

This equation can be transformed into

$$a(kk't) = a(k-\delta k, k'-\delta k, t-\delta t) +$$

$$-ik\left(v_{k'}-v_k\right)t\,\delta t\cdot a(kk't)$$

$$+\sum_{k''}\frac{E_1|\Delta E|\delta t}{\sqrt{2\hbar\omega_{\Delta k}\varepsilon V}}\left\{\left(\sqrt{N_q}\ldots-\sqrt{N_{q+1}}\ldots\right)a(k''k't)\right.$$

$$\left.-\left(\sqrt{N_q}\ldots-\sqrt{N_{q+1}}\ldots\right)a(kk''t)\right. \qquad (3.44)$$

. . .

which can be reduced to the same form of Eq.(3.1).

The application of the numerical techniques described earlier to Eq.(3.44) is currently under development.

REFERENCES

3.1 C.Jacoboni and L.Reggiani, Rev.Mod.Phys. 55, 645 (1985).

3.2 R.Rubinstein :"Simulation and The Monte Carlo Method", Wiley and Sons (1981).

FIGURE CAPTIONS

Fig.3.1:Exact solution (dotted line) and numerical solution (continuous line) as obtained following the procedure described in Sect.3.3, for uniform initial trial function (dashed line).

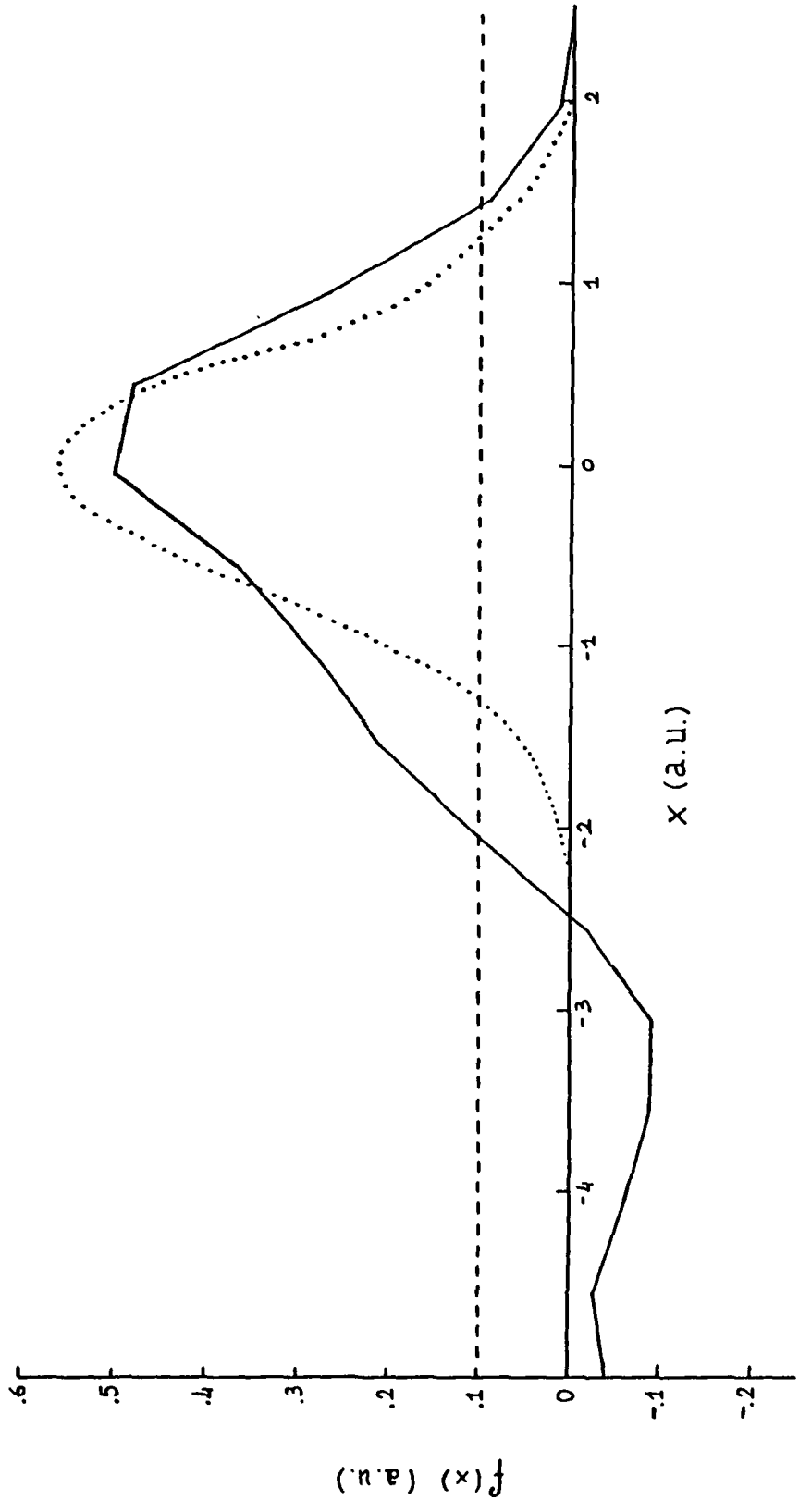

FIG. 3.1

4. FLUCTUATIONS OF CARRIER VELOCITY AND ENERGY IN STATIONARY AND TRANSIENT REGIMES

In recent times the analysis of velocity fluctuations of charge carriers in semiconductors in presence of high external electric fields has received renewed attention/4.1-4.12/. Modern microelectronics technology, in fact, has reached the submicron scale of miniaturization, at which a deeper insight into the physics of transport phenomena is required/4.13/,and fluctuations come to play an increasing role in the design and characterization of a device. Furthermore, a theoretical analysis of fluctuations at sufficiently high frequencies can yield significant information on the physical properties of the scattering sources present in the material under consideration and, more generally, on the microscopic interpretation of its transport properties.

Several papers have appeared on this subject in recent years. However no rigorous account has yet been given of the different sources for such fluctuations /4.14/ and very few results have been reported on transient fluctuations/4.15/.

We have performed a unified analysis of diffusion and noise problems obtained by means of the velocity autocorrelation function. This method can be used to describe both steady state (Sect.4.1) and transient

(Sect.4.2) phenomena, and also to analyze the different contributions to the diffusivity due to the different physical sources of fluctuations which arise in the presence of an applied electric field.

Results have been obtained with a Monte Carlo procedure for covalent (silicon) and polar (gallium arsenide) materials.

Furthermore, Monte Carlo calculations of hot-electron phenomena usually do not take into account interaction among carriers. On the other hand , a strong dependence of energy relaxation time on carrier concentration is observed at rather low carrier concentrations and it is thought to be due to carrier-carrier interaction.

An analysis of the influence of e-e scattering on the energy relaxation time is presented (Sect.4.3.1) through the energy autocorrelation function obtained from a Monte Carlo procedure which includes e-e interaction (Sect.4.3.2). Results will be shown for p-Ge and compared with experimental data (Sect.4.3.3).

4.1 Autocorrelation of velocity fluctuations, noise, and diffusion in steady-state conditions

4.1.1 Analysis of velocity fluctuations

Let us consider a homogeneous ensemble of carriers subject to a uniform static electric field $\vec{E}$ in steady-state conditions. Diffusion and noise are related to the stochastic velocity fluctuations $\delta\vec{v}(t)$ of each particle over the drift value $\vec{v}_d$. The mathematical quantity which describes the common origin of diffusion and noise is the autocorrelation function of velocity fluctuations, which, in one dimension, is defined as

$$C(t) = \langle \delta v(t') \cdot \delta v(t'-t) \rangle \quad , \qquad (4.1)$$

where the brackets indicate ensemble average, and the mean value, in steady- state conditions, is independent of t'. This quantity carries the information on how large these fluctuations are and how they decay in time.

C(t) is related to the diffusion coefficient D through the equation/4.16/:

$$D = \int_0^{+\infty} C(t)\, dt \qquad (4.2)$$

Thus D can be determined by Eq.(4.2) from the evaluation of C(t). It is worth noting that the calculation of C(t) is of interest in itself, because its analysis, as we shall see, yields a lot of physical information on the time evolution of the dynamic system under investigation.

Another important relation exists between the diffusion coefficient and the noise spectrum of velocity fluctuations, defined as

$$S_v(w) = \lim_{t\to+\infty} \frac{1}{T} \left\langle \left| \int_0^T \delta v(t)\, e^{i\omega t}\, dt \right|^2 \right\rangle \qquad (4.3)$$

Using the Wiener-Kintchine theorem [41] the well known relation

$$D = \frac{1}{2} S_v(0) \qquad (4.4)$$

is found. In order to describe the different origins of the various terms which can contribute to the diffusion process of carriers in semiconductors we shall consider a many-valley semiconductor with two types of valleys (this is the case, for example, of n-Si with the external field along a <100> direction).

Let us consider an electron that, at time t, is in a valley of type V(t) (V(t)=1 or 2) with energy between ϵ and $\epsilon+\Delta\epsilon$. We may then define:

v_d = drift velocity, i.e. mean velocity of all electrons;

$v_V(t)$ = valley drift velocity, i.e. mean velocity of all electrons in valley V(t);

$v_{\epsilon V}(t)$ = mean velocity of electrons in valley V with energy between ϵ and $\epsilon+\Delta\epsilon$.

The instantaneous velocity of each electron v(t) can then be written as the drift velocity plus a number of fluctuating terms/4.12/:

$$\vec{v}(t) = \vec{v}_d + \left[\vec{v}_v(t) - \vec{v}_d\right] + \left[\vec{v}_{ev}(t) - \vec{v}_v(t)\right] + \left[\vec{v}(t) - \vec{v}_{ev}(t)\right] =$$

$$= \vec{v}_d + \delta\vec{v}_v(t) + \delta\vec{v}_\epsilon(t) + \delta\vec{v}_k(t) \quad , \qquad (4.5)$$

where δv_v is the fluctuation associated with the drift velocity of the valley in which the electron is at time t, δv_ϵ is the fluctuation associated with the electron energy, and δv_k is the fluctuation associated with the electron momentum.

By using the expression in Eq.(4.1) the steady-state autocorrelation function becomes:

$$C(t) = \sum_{i,j} \langle \delta\vec{v}_i(t') \cdot \delta\vec{v}_j(t'+t) \rangle =$$

$$= \sum_{i,j} C_{ij}(t) \qquad (4.6)$$

where

$$C_{ij}(t) = \langle \delta\vec{v}_i(t) \cdot \delta\vec{v}_j(t'+t) \rangle \quad , \qquad (4.7)$$

and i,j=V, ϵ ,k. It has sometimes been implicitly assumed in the literature that the total noise due to velocity fluctuations is given by the sum of the three "diagonal" contributions C_{ii} in Eq.(4.6), at the origin of intervalley (C_{VV})/4.18,4.19/convective ($C_{\epsilon\epsilon}$)/4.20/, and thermal (C_{kk})/4.20/ noise, respectively. This restrictive assumption is correct only when the relaxation times of the various fluctuating terms have well differentiated values ,so that in calculating the "*off-diagonal* " terms one of the two fluctuations can be assumed as constant , while the other one averages to zero. In general, however,off-diagonal terms C_{ij} also contribute to the autocorrelation function and therefore to diffusion and noise. As an example, $C_{k\epsilon}$ (t) is the contribution to the autocorrelation of velocity fluctuations associated with correlations of momentum and energy fluctuations.

Due to the linearity of Eqs.(4.2) and (4.4) we can also associate specific terms in the autocorrelation function with corresponding terms in the diffusion constant and in noise, thus making explicit their physical origins.

4.1.2 The Monte Carlo Procedure

We use for the theoretical calculations a standard Monte Carlo procedure.

The evaluation of the autocorrelation function of δv

in steady-state conditions can be easily performed within the Monte Carlo simulation as follows. Let T be the time interval in which the autocorrelation function is to be sampled, which is usually taken as larger than the autocorrelation time (i.e. such that $C(t) \simeq 0$ for $t \geq T$). Then T is divided into a number M of intervals of duration $\Delta T = T/M$ in order to determine C(t) at the times

$$0 , \Delta T , 2\Delta T , \ldots , M\Delta T = T \quad .$$

During the simulation, the velocity of the sampled particle is recorded at the time values $i \cdot \Delta T$, $i = 0,1,2,\ldots$ When i becomes greater than M, the products

$$v(i\Delta T) \cdot v\left((i-j)\Delta T\right) , \quad j = 0,1,\ldots,M \qquad (4.8)$$

are evaluated for each i and j. Products corresponding to the same value of j are averaged over the simulation, thus obtaining

$$\overline{v(t) \cdot v(t + j\Delta T)} = C(i\Delta T) + v_d^2 \qquad (4.9)$$

(bar indicates time average), since in steady-state conditions the time average is equivalent to the ensemble average.

The noise spectrum can be easily obtained as a Fourier transform of C(t)/4.2/.

In order to determine the diffusion coefficient by means of a Monte Carlo simulation, the second central moment

$$M(t) = \left\langle \left[z(t) - \langle z(t) \rangle \right]^2 \right\rangle \qquad (4.10)$$

can be evaluated as a function of the simulation time t, where the average is performed over many different particles. For times larger than the initial transient, the time dependence of M(t) becomes linear and yields the diffusion coefficient as

$$D = \frac{1}{2} \frac{d}{dt} M(t) \qquad (4.11)$$

D can also be obtained from a numerical evaluation of the integral in Eq.(4.2) once C(t) has been obtained.

The physical models used in the calculations for Si and GaAs are those reported by Brunetti et al./4.21/ and Ruch/4.22/, respectively.

4.1.3 Results

Results have been obtained both for covalent (silicon case) and polar (GaAs case) materials. In order to simplify the complexity of the interpretation of these results let us

analyse the two cases separately.

Results for electrons in Si have been obtained with an applied electric field E=1ØkV/cm and a crystal temperature of 77 K. The simplest physical situation to discuss is that with the valleys symmetrically oriented with respect to the direction of the external field ($\vec{E}$//⟨111⟩).

Figs.4.1 and 4.2 report the autocorrelation function of velocity fluctuations and the different contributions, respectively, as analyzed in Sect.4.1.1, for the case $\vec{E}$// ⟨111⟩ . Within this analysis it is seen that a negative part in the total autocorrelation function is present, which is mostly due to the thermal contribution. Furthermore the off-diagonal term $C_{\epsilon k}(t)$ of the autocorrelation function, as defined in Eq.(4.6), also gives an appreciable contribution to the negative part, largely compensated by a positive contribution of $C_{k\epsilon}$. The particular form of these contributions is related to the energy dependence of the scattering mechanisms. In fact if , at a given time t, a positive fluctuation of electron momentum occurs, at a later time, due to the larger absorbed power, a positive fluctuation of energy is likely to occur; this,in turn, leads to an increase in the scattering efficiency, so there is a greater probability that a scattering will occur. Since each scattering is momentum randomizing, at larger times negative fluctuations of momentum will follow.

In order to connect this sequence of events to the shapes of the different terms C_{ij} (t), we need to relate energy fluctuations $\delta\epsilon$ to velocity fluctuations δv_ϵ .

Fig.4.3 shows $v_{\epsilon v}$ as a function of energy in Si for the same temperature and field considered above. It can be seen here that $v_{\epsilon v}$ is an increasing function of ϵ , so that a positive $\delta\epsilon$ will correspond to a positive δv_ϵ .

By collecting the above considerations, it can be understood why $C_{k\epsilon}$ is positive, $C_{\epsilon k}$ is negative, and C_{kk} is positive at smaller t and negative at larger t, with a minimum which is reached at times greater than the extrema of $C_{k\epsilon}$ and $C_{\epsilon k}$ (see Fig.4.2). In this case therefore the fact that the scattering probability is an increasing function of energy yields a negative contribution to longitudinal diffusivity through a negative part in C_{kk} and not through a negative convective contribution $C_{\epsilon\epsilon}$, which exibit a regular behaviour with a small negative part. Other off-diagonal terms are, in this case, much smaller.

Figs.4.1 and 4.4 report the autocorrelation function of velocity fluctuations and its different contributions, respectively, as analyzed in Sect.4.1.1 for $\vec{E}$// $\langle 100 \rangle$. In this case the different valleys have non- equivalent orientations with respect to the field direction, and therefore different components of the drift velocity along the direction of $\vec{E}$, so that the phenomenon of longitudinal

AD-A165 843 MONTE CARLO ANALYSIS OF QUANTUM TRANSPORT AND FLUCTUATIONS IN SEMICONDUCTORS(U) MODENA UNIV (ITALY) C JACOBONI 18 FEB 86 R/D-4260-EE DAJA45-83-C-0039 2/2

UNCLASSIFIED F/G 20/12 NL

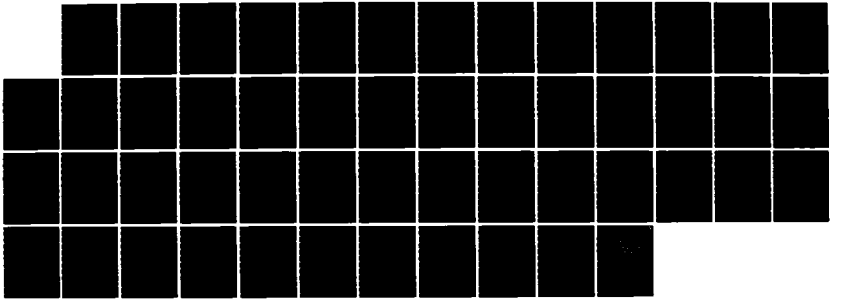

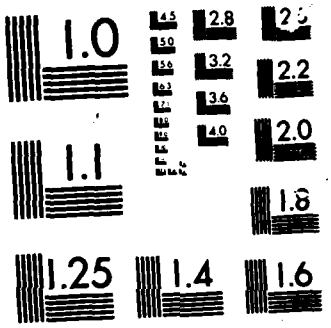

MICROCOPY RESOLUTION TEST CHART

intervalley diffusion occurs/4.21/. The intervalley contribution to C(t) is responsible for the long tail of the total autocorrelation function, absent for the case $\vec{E}//\langle 111\rangle$ (see Fig.4.1), since the intervalley transition time is the largest of the characteristic times of the process under investigation in these conditions of field and temperature. If we evaluate the integral of the intervalley contribution C_W, we find for the intervalley diffusion coefficient the value $D = 24 cm^2/sec$, which is very close to the difference $D^{\ell}_{100} - D^{\ell}_{111} = 21 cm^2/sec$ /4.21/.

The conclusion that such a difference is due to intervalley fluctuations is confirmed by the observation that the thermal and convective contributions to the total autocorrelation function are very similar for the two field orientations (see Figs 4.2 and 4.4).

In a transverse direction, for $\vec{E}//\langle 100\rangle$ velocity fluctuations are due only to thermal fluctuations ($v_v = v_{\epsilon v} = v_{cl} = 0$); their autocorrelation is always positive, since no energy transfer is associated with velocity fluctuations. For this reason D_t is always larger than D_ℓ, when the scattering efficiency is an increasing function of ϵ.

Fig.4.5 shows the noise spectral density $S_v(\omega)$ for the case of $\vec{E}//\langle 100\rangle$ discussed above. Again, the peculiar shape of the total $S_v(\omega)$ can be understood from the analysis of the partial contributions, also shown in

Fig.4.5. The white-noise value of the total spectrum, corresponding to a diffusion coefficient of 41 cm^2/sec , is strongly influenced by the large intervalley contribution (D_{vv} =31 cm^2/sec). This term shows the most rapid decrease at increasing frequencies due to the largest relaxation time of the intervalley velocity fluctuations. The thermal term gives a relatively small contribution(D_{tt}=14 cm^2/sec) to the white-noise level, as an effect of the cancellation of the negative and positive parts of C_{tt}, and has a bump, due to the strong oscillation of C_{tt}. The convective contribution, with a white-noise level corresponding to $D_{\epsilon\epsilon}$=10cm^2/sec, is present with a monotonically decreasing behaviour, and is always positive. The off-diagonal terms $S_{k\epsilon}$ and $S_{\epsilon k}$ have similar shapes of opposite signs; their cumulative contribution, which is relatively small, is negative at low frequencies, corresponding to a negative contribution to diffusivity, and becomes positive at high frequencies.

The total noise spectrum corresponding to the sum of the different terms seen above shows a non-Lorentian behaviour with a fast initial decrease due to the decrease of the intervalley term followed by a bump due to the thermal contribution and by the final $1/\omega^2$ dependence. Due to the high frequencies involved, it may be difficult to detect experimentally the maximum of $S_v(\omega)$ at 800 GHz. In experiments however , it must be taken into account that an

initial decrease of $S_v(\omega)$ after a white-noise level does not indicate the cut-off of velocity fluctuations, but rather yields information on the intervalley relaxation time.

Results consistent with the above interpretation have been obtained with calculations performed at other temperatures and fields. In particular, for T=77 K and E=200 V/cm along a $\langle 100 \rangle$ and a $\langle 111 \rangle$ directions, agreement has been found with experimental data of Bareikis /4.23/,as shown in Fig.4.6.

Results for electrons in GaAs have been obtained with an applied electric field E=10kV/cm and a crystal temperature of 300 K.

Fig.4.7-a reports the autocorrelation function of velocity fluctuations together with its three diagonal terms. The thermal fluctuations at the chosen field strength are much higher than for the case of Si, owing to the higher electron energy.

Fig.4.7-b reports the off-diagonal terms. They are all of the same order of magnitude, but much smaller than the thermal contribution, so that in this part of the figure a different vertical scale has been used.

The interpretation of the diagonal terms, as well as of the off-diagonal terms $C_{\epsilon t}$ and $C_{t\epsilon}$, is similar to that given for the case of Si. Fig.4.8 shows, in fact, that v_ϵ is a

monotonous function of energy also for the case of GaAs. This figure also shows two interesting features. By increasing the field above threshold for negative differential mobility, the whole v_ϵ curve (not only its high-energy part) is reduced, due to the randomizing effect of intervalley scattering. The effect is related to the intervalley collisions with the final $\vec{k}$ in the central valley with direction opposite to the electric force/4.24/. Furthermore, at energies above threshold for intervalley scattering, the curve v_ϵ increases more sharply, because electrons enter this region of energy mainly because of acceleration due to the field.

In order to discuss the results for the other off-diagonal terms, we shall refer to the succession of electron states described in Ref.4.24. Electrons in the upper valley will eventually be scattered in the negative half $\vec{k}$-space of the lower valley into a state with high energy; as an effect of the field, their energy will first decrease, and then increase until the electron will again be scattered into the upper valley, in this way beginning a new cycle. Therefore, when an electron is in the "slow" upper valley ($\delta v_V < 0$), a positive fluctuation of energy will most probably follow, corresponding to a positive δv_ϵ, with a negative $\vec{k}$ in the central valley. This is the main reason for having $C_{V\epsilon}$ negative and C_{Vk} positive. When $\delta\vec{k}$ (and

consequently $\delta\vec{v}_k$) is positive, a large energy will follow ($\delta v_\epsilon > 0$) and the electron will lie predominantly in the slow valley ($\delta v_v < 0$) until its energy has been decreased by successive intervalley scatterings; when, instead, $\delta\vec{k}$ is negative ($\delta v_k < 0$), then the energy will be decreased by the field action ($\delta v_\epsilon < 0$) and the electron will lie in the "fast" valley ($\delta v_v > 0$) until it again reaches an energy comparable with that necessary to emit an intervalley phonon. This explains why C_{kv} and $C_{\epsilon v}$ are negative.

Fig.4.9 shows the spectral densities calculated from the autocorrelation functions shown in Fig.4.7. $S_{v\epsilon}$ and $S_{\epsilon v}$ are smaller than the other contributions and have not been reported for the sake of clarity.

As regards the noise spectrum, at high frequencies the thermal contribution S_{kk} is dominant, while for the white noise, owing to the large cancellation of the positive and negative part of C_{kk}, S_{kk} becomes comparable with other terms.

4.2 Transient Autocorrelation of Velocity Fluctuations and Diffusion

4.2.1 Transient correlations

The diffusion process of a carrier ensemble comes from

the particle space-velocity correlations which arise during the evolution in time of the system.

Starting from an initial condition in which the particle positions and velocities are totally uncorrelated, the process which occurs during the time necessary for setting up the correlations will be defined as the correlation transient. Furthermore, when a high electric field is applied at a certain time to the electron ensemble, the transport process itself must pass through a transient regime which is necessary for attaining the stationary distribution $f(\vec{k})$ in $\vec{k}$-space. This process will be called transport transient.

In what follows we shall discuss how these two different transients can be analysed separately, but simultaneously, and how their effects influence the transient of the diffusivity of the electron ensemble.

The definition of the transient diffusion coefficient has been given by a generalization of Eq.(4.11) to arbitrary small times /4.25-4.27/:

$$D(t) = \frac{1}{2} \frac{d}{dt} \left\langle \left(z(t) - \langle z \rangle_t \right)^2 \right\rangle \qquad (4.12)$$

where z(t) is the space position of a carrier at time t along the z-direction parallel to $\vec{v}_d$.

This generalization can be put in an equivalent form in

terms of the autocorrelation function, which is easily interpretable from a physical point of view. By using

$$Z(t) = Z(0) + \int_0^t v(t)\,dt \qquad (4.13)$$

in Eq.(4.12)we have:

$$D(t) = \frac{1}{2}\frac{d}{dt}\left\{\langle \delta Z^2(0)\rangle + 2\langle \delta Z(0)\int_0^t \delta v(t')\,dt'\rangle + \right.$$

$$\left. + \int_0^t dt' \int_0^t dt'' \langle \delta v(t')\cdot \delta v(t'')\rangle\right\} =$$

$$= \langle \delta Z(0)\cdot \delta v(t)\rangle + \int_0^t dt' \langle \delta v(t)\cdot \delta v(t')\rangle \qquad (4.14)$$

If there is no correlation between the initial positions and velocities of the particles, Eq.(4.14) becomes:

$$D(t) = \int_0^t d\tau\, C_t(\tau) \qquad (4.15)$$

with

$$C_t(\tau) = \langle \delta v(t)\cdot \delta v(t-\tau)\rangle, \quad 0 \le \tau \le t \qquad (4.16)$$

where we have put in Eq.(4.15): $\tau = t' - t$. Eq.(4.15) reduces to Eq.(4.2) in steady- state conditions ($t \to \infty$).

By comparison of these two expressions, we see that in the present case: (i) the integration interval does not

extend to +∞ but toward the past, back only as far as the initial conditions; this finite integration brings about the effect of correlation transient;

(ii) the autocorrelation function to be integrated in the transient analysis (Eq.4.16) is not time independent; it is given by the specific ensemble average at a particular time, and its shape provides information about the transport transient.

4.2.2 The Monte Carlo Procedure

The transient autocorrelation function $C_t(\mathcal{E})$, also called two-time autocorrelation function /4.15/ can be calculated with a Monte Carlo procedure through the simulation of the dynamics of an ensemble of electrons. At fixed times $0, \Delta t, 2\Delta t, \ldots$, the direct calculation of the velocity fluctuations is performed with respect to the mean value, calculated at the same time over the carrier ensemble. The products $v(i\Delta t) \cdot v(j\Delta t)$, $j=0,1,\ldots,i$ are then averaged over the ensemble and they give i+1 values of the transient autocorrelation function at the time $t=i\Delta t$.

The analysis of the various contributions to the autocorrelation function (see Eq.(4.6)), according to the separation in Eq.(4.5), can also be obtained for the transient case in a similar way.

The present analysis holds also if the field is

switched on at a time t_s larger than the time t=Ø of the initial conditions /4.28/. In this case the effect of the transport transient is separated in time from the initial correlation transient of the zero-field diffusion (see the next section).

4.2.3 Results

As application of the general theory outlined in the previous section, we now discuss the results obtained for few special examples which contain the significant features of most of the interesting cases. All the results have been obtained with the Monte Carlo technique for electrons in Si with the silicon model referenced to in the previous section.

Fig.4.1Ø presents results for the second central moment, the transient longitudinal diffusion coefficient, obtained with Eq.(4.12), and the mean velocity, as functions of time for electrons in Si with $\vec{E}_{111}$ =1Ø kV/cm. The following initial conditions have been taken: electrons are randomly situated in one of the six valleys with equal probability; the velocities are chosen according to an equilibrium Maxwellian distribution, and the electrons are all positioned at r=Ø.

Fig.4.1Ø shows that the second central moment first increases quadratically with time, as predicted by ballistic

behaviour. At intermediate times (Ø.2-1. psec) an irregular behaviour is exibited by the diffusivity: a tendency to level off, followed by an overshoot ($t \simeq Ø.8$ psec). Then, at sufficiently long times, the second central moment shows the linear dependence on time with the slope corresponding to the steady-state diffusion.

This behaviour is due essentially to the combined action of the acceleration impressed by the external field and of the dissipation of energy and momentum associated with intervalley scattering. At the very beginning the field accelerates the electron gas, and all the particles move toward the region of energy where intervally emission becomes possible. In this interval of time (Ø-Ø.2 psec) we have the ballistic regime, in which both mean velocity and diffusivity increase linearly with time (see Figs.4.1Ø-c and b). The fastest electrons will then undergo intervalley scattering, becoming in this way very slow ; as a consequence mean velocity and diffusivity tend to level off ($t \simeq Ø.5$ psec). Later, as an effect of the scattering, we have a separation between fast electrons (those which have not yet undergone scattering) and slow electrons (which did undergo scattering), which causes a fast increase in the diffusivity (see Fig.4.1Ø-b) and a decrease in the mean velocity (see Fig.4.1Ø-c) after its maximum value ($t \simeq Ø.8$ psec). Finally, due to the randomness of the scattering,

the randomized steady distribution of velocities will be set up, and both $\langle v \rangle$ and D reach the steady-state value; the steady diffusivity is lower than the overshoot value because each particle becomes, in steady-state conditions,alternatively slow and fast, with a reduction of the spreading rate at long times,as indicated by the negative part in the stationary autocorrelation function.

As previously noticed, the results on transient diffusion can be analysed and understood in terms of the transient autocorrelation function $C_t(\tau)$. The examples presented below (Figs.4.11 and 4.12) refer to the silicon case with E=10 kV/cm. However here the field has been chosen along a $\langle 100 \rangle$ direction in order to add in the discussion the effect of the intervalley contribution to the diffusivity.

Fig.4.11 shows the transient autocorrelation function, as a function of τ at various times t; the same initial conditions used in Fig. 4.10 have been taken. Each of these curves is interrupted at $\tau = t$ when the correlation with the initial conditions is reached. The area under each curve gives the corresponding value at time t of the transient diffusion coefficient. At very short times this area is very small both because $C_t(\tau)$ starts from low values, and because it is interrupted at short τ. The first effect is a consequence of the transport transient , the electrons being

still "cold", while the second effect is present because at small times the correlations are not yet established (correlation transient). As t increases, the area reaches larger values, and it is maximum when the positive part of $C_t(\tau)$ is totally present, and a negative part is not yet present. This leads to the overshoot of the transient diffusivity. When negative correlations are established, D(t) decreases toward the steady-state value, which is attained when the shape of $C_t(\tau)$ reproduces the steady-state function and the integral of the autocorrelation function is extended to all significant values of τ .

It is particularly interesting to reproduce the same analysis for the intervalley contribution alone. Fig.4.12 shows the transient autocorrelation function $C_t(\tau)$ for the intervalley velocity fluctuations $\delta v_V(t)$, defined in Sect.4.2.1, as a function of for various times t. The most striking aspect of this set of curves is the presence of a bump which is shifted toward a greater value of τ, as t increases. This phenomenon is clearly due to the velocity overshoot in the two types of valleys which increases the value of $\delta v(t)$ with respect to the steady state. As t increases, this overshoot recedes more and more in the past, so that it is seen at larger correlation times until it vanishes, when any memory of the overshoot effect is lost.

The overshoot of the GaAs diffusivity /4.29/can be

analysed in a similar way, and a negative part of the transient autocorrelation function prevails over the positive one at the times when D is found negative/4.29/. This strong negative correlation is a consequence of the electron transfer back and forth from central to upper valleys, as discussed above.

As a final result, we report in Fig.4.13 an analysis of the transient diffusivity in a case in which the electric field is applied after the onset of the zero-field correlations. Before application of the field, the diffusivity slowly reaches the steady-state value in about 10 psec. When the electric field is applied, a transport transient occurs, with heating of the carriers, on a shorter time scale(in about 2 psec); during this time new correlations are established and the diffusivity reaches the new lower steady value, passing through a minimum with a region of negative values. This negative region is in great contrast with the overshoot of D seen for the case in Fig.4.10. This can be explained by considering that the first electrons which undergo intervalley scattering after the field application are the fastest electrons in the direction of the field; during the first part of the process (zero-field correlation transient) the distributions of carriers have fully developed the space-velocity correlations at the basis of the diffusion process, so that

a slowing down of the fastest particles due to intervalley scattering produces a shrinking of the space distribution, corresponding to the negative D. It may be useful to compare the behaviour of D after the onset of the field in Fig.4.13 with fig.4.10-b in order to appreciate the influence of the initial conditions in the transient diffusion.

4.3 Autocorrelation of Energy Fluctuations and Energy Relaxation in presence of carrier-carrier interaction

4.3.1 The influence of carrier-carrier interaction on the energy relaxation

Monte Carlo calculations of hot-electron phenomena in semiconductors seem to indicate that e-e interaction introduce, in general, small corrections to the transport quantities even at high carrier concentrations /4.30/.

On the other hand, a strong dependence of energy

relaxation time on carrier concentration in warm electron conditions is observed at rather low carrier concentrations (10^{15} -10^{16} cm-3 in different semiconductors) /4.31-4.33/.

The experimental data are obtained when the electron concentration is changed in two different ways: namely, by doping and compensating. In the latter case the electron concentration decreases when that of the impurities increases. Therefore the effect cannot be ascribed to impurity scattering, and consequently it is thought to be due to the interaction among carriers. For a detailed discussion of the experimental data see Refs.4.34,4.35.

It is well known that e-e scattering, which is energy and momentum conserving, cannot have a direct influence on the physical mean quantities relative to the carrier ensemble. However the presence of carrier interaction can alter the probability of occurrence of other lattice scatterings, especially those with a well defined threshold of activation (e.g. emission of an optical or intervalley phonon)/4.36,4.37/.

A previous comparison between experimental and theoretical results was performed in Ref.4.37 by means of a

Monte Carlo simulation of a carrier ensemble interacting through a Coulomb field. The theoretical effect was weaker than the experimentally observed.

A different possible approach is to consider the interaction through two-carrier collisions. When a screened Coulomb potential has been used the collisions have been found to contribute to carrier distribution and correlation functions /4.38-4.40/, but a comparison with experimental energy relaxations has not been made.

In order to determine the energy relaxation time τ_ϵ from Monte Carlo simulation, we have proceeded in two different ways.

The dependence of the carrier mean energy $\langle \epsilon(t) \rangle$ on time after the field has been switched on is recorded; under warm-electron conditions, corresponding to weak deviations from the thermal equilibrium, the above dependence can be approximated as follows/4.35/:

$$\langle \Delta\epsilon(t) \rangle = \langle \Delta\epsilon_\infty \rangle \cdot \left(1 - e^{-t/\tau_\epsilon}\right) \quad (4.17)$$

where $\langle \Delta\epsilon(t)\rangle = \langle \epsilon(t)\rangle - \frac{3}{2}K_B T$ is the extra energy at time t, and $\langle \Delta\epsilon_\infty \rangle$ is its value in stationary conditions. From a best fit of the simulation data with Eq(4.17) a value for can be obtained.

The above procedure is subject to the criticism that the electron energy relaxation is itself a function of time in the transient regime, during which the carrier distribution is heated up, even though this effect should not be important for the dependence of τ_ϵ on carrier concentration.

The relaxation time can be well defined only in stationary conditions, and it can be obtained by means of the autocorrelation function of energy fluctuations from

$$\tau_\epsilon = \frac{1}{\overline{(\delta\epsilon(t))^2}} \cdot \int_0^{+\infty} d\eta \; \overline{\delta\epsilon(t)\cdot\delta\epsilon(t+\eta)} \qquad (4.18)$$

where $\delta\epsilon$ is the energy fluctuation of the ensemble and — indicates time average, respectively.

4.3.2 The Monte Carlo Procedure

Theoretical calculations for the energy relaxation time through the above-mentioned approach and a comparison with the experimental data have been performed for p-Ge. The choice falls on these experiments for two reasons. Firstly the uncontrolled impurity background was low in these measurements, thus in the range of controlled concentrations of $10^{13} - 10^{15}$ cm-3 the ionized impurity scattering can be neglected /4.41/. Next, the models for band structure and lattice scattering for this material allow a simple appproximation which gives satisfactory results /4.30/.

The model of p-Ge used hereafter is a widely used one /4.30/: only one heavy-mass subband is taken into account which is considered spherical and parabolic with $m=0.34m_0$. Optical phonons are considered dispersionless ($\hbar\omega_0$ =0.037 eV). The deformation potential consta nt D_{ac} is taken to be 9x10**8 eV/cm. Nonelasticity of acoustic scattering is included in the way used in Ref.4.42; sound velocity and acoustic deformation potential are chosen as 3.85 x 10**5 cm/sec and 3.25 eV, respectively. The crystal temperature has been chosen as 100 K in order to allow the comparison

with the experimental data.

The Ensemble Monte Carlo procedure used for the calculations has been modified to include e-e interaction in the following way. Starting from an initial equilibrium carrier distribution, a uniform and constant electric field is switched on, and carrier dynamics is simulated during a time step short enough as compared to the energy and momentum relaxation times, and even shorter than the time between two successive interparticle collisions.

Carrier-carrier collisions are introduced through a spherical screened Coulomb potential

$$V(\vec{r}) = \frac{e^2}{4\pi\varepsilon\varepsilon_0}\,\frac{1}{r}\,e^{-\beta r} \qquad (4.19)$$

where r is the distance, ε is the relative dielectric constant, β the inverse screening depth, which depends on carrier density n. The Debye thermal-equilibrium value of β has been used, since warm-electron conditions have been considered.

The scattering rate for two given carriers is as follows

/4.38/:

$$\lambda(\vec{g}) = \frac{m e^2 K_B T}{4\pi \hbar^3 \varepsilon \varepsilon_0 n} \quad \frac{g^2}{g^2+\beta^2} \qquad (4.20)$$

where $\vec{g} = \vec{k}_c - \vec{k}$ is the wavevector difference of the colliding particles, $\vec{k}$ and $\vec{k}c$ are the wavevectors of the test carrier and the counterpart electron before their collision.

The total scattering rate for an electron with wavevector $\vec{k}$ is given by

$$P_{ee}(\vec{k}) = \frac{m e^2 K_B T}{4\pi \hbar^3 \varepsilon \varepsilon_0} \int \frac{g}{g^2+\beta^2} f(\vec{E}_c)\, d\vec{E}_c \qquad (4.21)$$

Since the distribution in $\vec{k}$-space of the counterparts $f(\vec{k}_c)$ is not known a priori, the following rejection technique has been used. A self scattering internal to the e-e interaction is introduced by substituting $g/(g^2+\beta^2)$ in Eq.(4.21) with its maximum value $1/2\beta$. In this way $P_{ee}(\vec{k}) + P_{ee}^{self}(\vec{k})$ results to be:

$$P_{ee}^{1} = \frac{m \cdot e^4}{8\pi (\varepsilon\varepsilon_0)^2 \hbar^3 \beta^3} \qquad (4.22)$$

This new e-e total scattering probability is introduced among the other mechanisms. When an electron attempts an intercarrier collision, a counterpart carrier is selected at random from the particle distribution. If $\vec{g}$ is the wavevector difference between the Monte Carlo electron and the counterpart, and a random number r results to be less than $2\beta g/(g^{**2}+\beta^{**2})$, the e-e collision is accepted. In this case the final states of both electrons involved into the scattering process are selected according to the differential cross section relative to the potential in Eq.(4.19) and taking into account energy and momentum conservations.

In doing so the state of the Monte Carlo electron is changed at the time of the collision; the state of the counterpart is changed at the time in which its simulation was suspended. Through this procedure the distribution of the counterpart carriers is not exactly syncronous with the

simulation time of the Monte Carlo electron, but this difference is not relevant if the time-step duration Δt is smaller than the time between two interparticle collisions.

4.3.3 Results

Figs.4.14 and 4.15 show typical results obtained with the Monte Carlo simulation following the two approaches indicated in Sect.4.3.1.

Fig4.16 shows the dependence of τ_ϵ on the electric field at a fixed concentration. At the highest field values considered here the condition of warm-electron regime may not be fulfilled, but these fields have been considered here only to check the consistence of the physical picture.

It can be seen here that the effect of e-e interaction is to reduce τ_ϵ.

This effect can be explained through the general considerations reported in Sect.4.3.1. At low fields few carriers have enough energy to emit optical phonons, due to the low heating involved, while the majority of carriers interact with acoustic phonons in a nearly elastic way.

Intercarrier collisions change the effectiveness of the interaction with the lattice. In particular, an essential contribution to the energy losses comes from two passive carriers (that is having energy less than $\hbar\omega_0$) if, during their collision, one carrier gains enough energy for a subsequent emisson of an optical phonon.

As a general confirmation of this picture, Fig.4.17 shows the energy dissipation rate , normalised to the value without e-e interaction, for the optical phonon scattering as a function of the electric field at a carrier concentration of $1.\times 10^{15}$ cm-3. It can be seen that at low electric fields the rate of dissipation is substantially enhanced with respect to the equilibrium case, due to the increase of the "active" carriers, as effect of the e-e scattering. At the highest fields, due to the heating, more carriers are active also without e-e scattering, and the quantities in Figs.4.16 and 4.17 become practically insensitive to the interaction.

Finally in Fig.4.18 we report the normalised energy relaxation time as a function of carrier concentration compared with the experimental data of Ref.431.

The two theoretical techniques do not show relevant

discrepancies in the normalised values. Even though the theoretical results are affected by a certain statistical error, there is no doubt that the effect theoretically predicted is less than the one observed in the experiments, as previously found.

E-e interaction, even trated as two-particle collisions cannot account for the experimental enhancement of energy relaxation, and more sophisticated mechanisms must be invoked.

REFERENCES

4.1 G.Hill,P.N. Robson, and W.Fawcett, J.Appl.Phys. 50, 356,(1979).

4.2 R.Fauquembergue,J.Zimmermann,A.Kaszynski, E.Constant, and G.Microondes,J.Appl.Phys. 51,1065 (1980).

4.3 D.K.Ferry, Phys.Rev.Lett. 45,758 (1980).

4.4 R.O.Grondin,P.A.Blackey,J.R.East, and E.D.Rothman, IEEE Trans.Electron Devices ED-28, 914 (1981).

4.5 R.Brunetti,C.Jacoboni,and L.Reggiani, Proc. III Int.Conf. on Hot Carriers in Semiconductors, J.Phys. (Paris) Coll.C7 Suppl.n.10, 42, 117 (1981).

4.6 V.Bareikis,A.Galdikas,R.Miliusyte,V.Victoravicius, Proc. 6-th Int.Symposium on Noise in Physical Systems, National Bureau of Standards Special Publication n.614 (U.S. GPO, Washington D.C. (1981),p.406.

4.7 V.Bareikis,A.Galdikas,R.Miliusyte,J.Pozhela,V.Viktoravichius,Proc. III Int.Conference on Hot Carriers in Semiconductors, J.Phys.(Paris) Coll.C7 Suppl.n.10, 42, (1981).

4.8 J.Pozhela,Editor, Hot Electron Diffusion (in Russian) , Mosklas,Vilnius(1981).

4.9 A.Matulionis,J.Pozhela,and E.Starikov, Sov. Phys. Semicond.16, 388 (1982).

4.10 M. Deb Roy and B.R. Nag, Appl. Phys. A26, 131 (1981).

4.11 M. Deb Roy and B.R. Nag, Appl. Phys. A28, 195 (1982).

4.12 R.Brunetti and C.Jacoboni, Phys. Rev. Lett. 50, 1164 (1983).

4.13 See, for example, IEEE Trans. Electron Devices ED 28 (special issue)(1981); Proc. NATO-ASI"Physics of Submicron Semiconductor Devices", S.Miniato(Italy) 10-23 July 1983, in press.

4.14 A preliminary report on the steady-state analysis presented here has been given in Ref.4.12.

4.15 P.Lugli,J.Zimmermann, and D.K.Ferry,Proc.III Int. Conference on Hot Carriers in Semiconductors, J. Phys.(Paris) Coll.C7 Suppl.n.10 42,103 (1981).

4.16 F. Reif, Fundamentals of Statistical and Thermal Physics, Mc Graw Hill, New York (1965).

4.17 C. Kittel, Elementary Statistical Physics, Wiley , New York (1958).

4.18 P.J.Price, J. Appl. Phys. 31, 124 (1960).

4.19 W.Shockley, J.A. Copeland, and R.P. James, in Quantum Theory of Atoms, Molecules and The Solid State, Academic Press, New York (1966).

4.20 P.J. Price, in Fluctuation Phenomena in Solids, Ed. by Burgess,Chapt.6, Academic Press, New

York (1965).

4.21 R.Brunetti, C. Jacoboni, F. Nava, L. Reggiani, G. Bosman, and R.J.J.Zijlstra, J. Appl. Phys. 52, 1713 (1981).

4.22 J.G. Ruch, IEEE Trans. Electron. Devices, ED 19 652 (1972).

4.23 V. Bareikis, private communication.

4.24 W.Fawcett,D.A.Boardman and S.Swain,J. Phys. Chem. Solids 31, 1963 (1970);

4.25 A. Alberigi-Quaranta, V. Borsari, C. Jacoboni, and G.Zanarini, Appl.Phys. Lett. 22, 103 (1973).

4.26 D.K. Ferry and J.R. Barker, J. Appl. Phys. 52, 818 (1981).

4.27 L. Reggiani, R. Brunetti, and C. Jacoboni, Proc. III Int. Conf. on Hot Carriers in Semiconductors, J.Phys.(Paris) Coll. C7 Suppl. n.10, 42, p.111 (1981).

4.28 E. Constant and B. Boittiaux, Proc. III Int. Conf. on Hot Carriers in Semiconductors, J.Phys.(Paris) Coll. C7 Suppl.n.10, 42, 73 (1981).

4.29 B.Boittiaux,E.Constant,L.Reggiani,R.Brunetti,and C.Jacoboni, Appl.Phys.Lett. 40, 407 (1982).

4.30 C.Jacoboni and L.Reggiani, Rev.Mod.Phys. 55, 645 (1983).

4.31 A.P.Boltaev and N.A.Penin, Sov.Phys.Sem.11, 1322

(1977).

4.32 V.Dienys and Z.Kankleris, Phys.Stat.Sol.(b)67, 317 (1975).

4.33 S.P.Ashmontas and L.E.Subacius, Sov.Phys.Sem.17, 583 (1983).

4.34 .Dienys and Z.Kankleris, Electron-electron scattering in covalent semiconductors, in: Electrons in Semiconductors, Vol.I ed. J.Pozhela, Mosklas, Moskow, pp.59-86 (1978).

4.35 V.Dienys, Z.Kankleris and Z.Martunas: Electrons in Semiconductors,Vol.4, ed.J.Pozhela, Mosklas, Moskow (1983).

4.36 I.B.Levinson and G.E.Mazuolyte, Sov.Phys. JETP, 697 (1966).

4.37 C.Jacoboni, Proc.XIII Int.Conf.Semic., ed. E.Fumi, Marves, Rome,pp.1195-1205 (1976).

4.38 A.Matulionis,J.Pozhela and A.Reklaitis, Sol.State Commun., 16, 1133 (1975).

4.39 M.Takenaka and M.Inoue, J.Phys.Soc.Japan 47,861 (1979).

4.40 P.Lugli and D.K.Ferry, Proc.XVI Int.Conf.Semic. ed J.Averous, pp.251,256 North Holland, Amsterdam (1982).

4.41 L.Reggiani, Phys.Rev.b17, 2800 (1978).

4.42 C.Canali,C.Jacoboni,F.Nava,G.Ottaviani, and A.Alberigi Quaranta,Phys.Rev.b12, 2265 (1975).

FIGURE CAPTIONS

Fig.4.1: velocity autocorrelation function for electrons in Si, as obtained from a Monte Carlo simulation, at 77 K for E=10kV/cm applied along a ⟨100⟩ (continuous line) and ⟨111⟩ (dashed line) directions, respectively

Fig.4.2: a) autocorrelation function of thermal and convective fluctuations for electrons in Si at 77 K and E =10kV/cm (see Sect.4.1.1); b) off-diagonal terms $C_{\epsilon k}$ and $C_{k\epsilon}$ which contribute significantly to the total velocity autocorrelation function for the case shown in a).

Fig.4.3: mean velocity (continuous line and left scale) and distribution function (dashed line and right scale), as functions of energy for electrons in Si at the indicated temperature and field.

Fig.4.4: a) autocorrelation function of thermal, convective and intervalley fluctuations for electrons in Si at 77 K and E =10kV/cm (see Sect.4.1.1); b) off-diagonal terms $C_{\epsilon k}$ and $C_{k\epsilon}$ which contribute to the total autocorrelation function for the case shown a).

Fig.4.5: spectral density of velocity fluctuations and its

components for electrons in Si at the indicated temperature and field obtained as Fourier transforms of the autocorrelation function shown in Fig.4.1 and 4.4. The lettering of the curves is defined in the text.

Fig.4.6: spectral density of velocity fluctuations for electrons in Si at 77 K and E=200 V/cm along a ⟨100⟩ and a ⟨111⟩ directions. Points refer to experimental data of Bareikis /4.23/ and lines refer to Monte Carlo calculations.

Fig.4.7:(a) autocorrelation function of velocity fluctuations and its diagonal terms,and (b) off-diagonal terms for the case of electrons in GaAs at the indicated temperature and field. In (b) a different vertical scale has been used.

Fig.4.8: mean velocity (continuous lines and left scale) and distribution function (dashed lines and right scale) as functions of energy for electrons in the central valley in GaAs at T=300K. The numbers on the curves indicate the field strength in kV/cm.

Fig.4.9: spectral density of velocity fluctuations and its components for electrons in GaAs at the indicated temperature and field obtained as Fourier transforms of the

autocorrelation functions shown in Fig.4.7. The lettering on the curves is defined in the text.

Fig.4.10: second central moment (a), longitudinal diffusion coefficient (b), and mean velocity (c) as functions of time for electrons in Si at 77 K and E=10 kV/cm along a ⟨111⟩ direction.

Fig.4.11: transient velocity autocorrelation function vs. correlation time τ at fixed times t (reported in psec over each curve in the figure) for electrons in Si at 77 K and E=10kV/cm along a ⟨100⟩ direction. Each curve is interrupted at τ=t when the correlation with the initial conditions is reached. The stationary autocorrelation function (continuous line) is shown for comparison.

Fig.4.12: transient intervalley autocorrelation function vs. correlation time at fixed times t (reported in psec over each curve in the figure) for electrons in Si at 77 K and E=10 kV/cm along a ⟨100⟩ direction. Each curve is interrupted at τ=t, when the correlation with the initial conditions is reached. The stationary intervalley autocorrelation function (t→∞) is shown for comparison.

Fig.4.13: transient diffusivity as a function of time for

electrons in Si at 77 K, in a physical situation in which a field E_{111} =10 kV/cm is switched on at time t_S =9.57 psec after the initial conditions (t=0) of uncorrelated particles.

Fig.4.14:Carrier heating during the transient transport with field E=70 V/cm and T=100 K. The continuous curves have been obtained by a best fit of the simulation data with Eq.(4.17). Numbers indicate carrier concentrations in units of 10**15 cm-3. Points indicate simulation data for n=5x10**15 cm-3.

Fig.4.15:Autocorrelation function of energy fluctuations in steady-state conditions without (closed circles) and with (open circles) e-e interaction for a concentration n=5x10**14 cm-3. T=100 K; E=70 V/cm.

Fig.4.16:Relative energy relaxation time as a function of field strength at a carrier concentration n=1x10**15 cm-3. Triangles and circles refer to data obtained by fitting the transient heating and with the energy autocorrelation function in steady-state, respectively. T=100 K.

Fig.4.17:Relative energy loss through optical phonons at a

carrier concentration n=1x10**15 cm-3, as a function of field strenght. T=100 K.

Fig.4.18:Relative energy relaxation time as a function of carrier concentration . Triangles and closed circles refer to data at a field strenght E=70 V/cm obtained by fitting the transient heating and with the energy autocorrelation function, respectively. The cross indicates values obtained at E=20 V/cm with the two techniques, indistinguishable in this scale. Open circles refer to the experimental data in Ref.4.31.

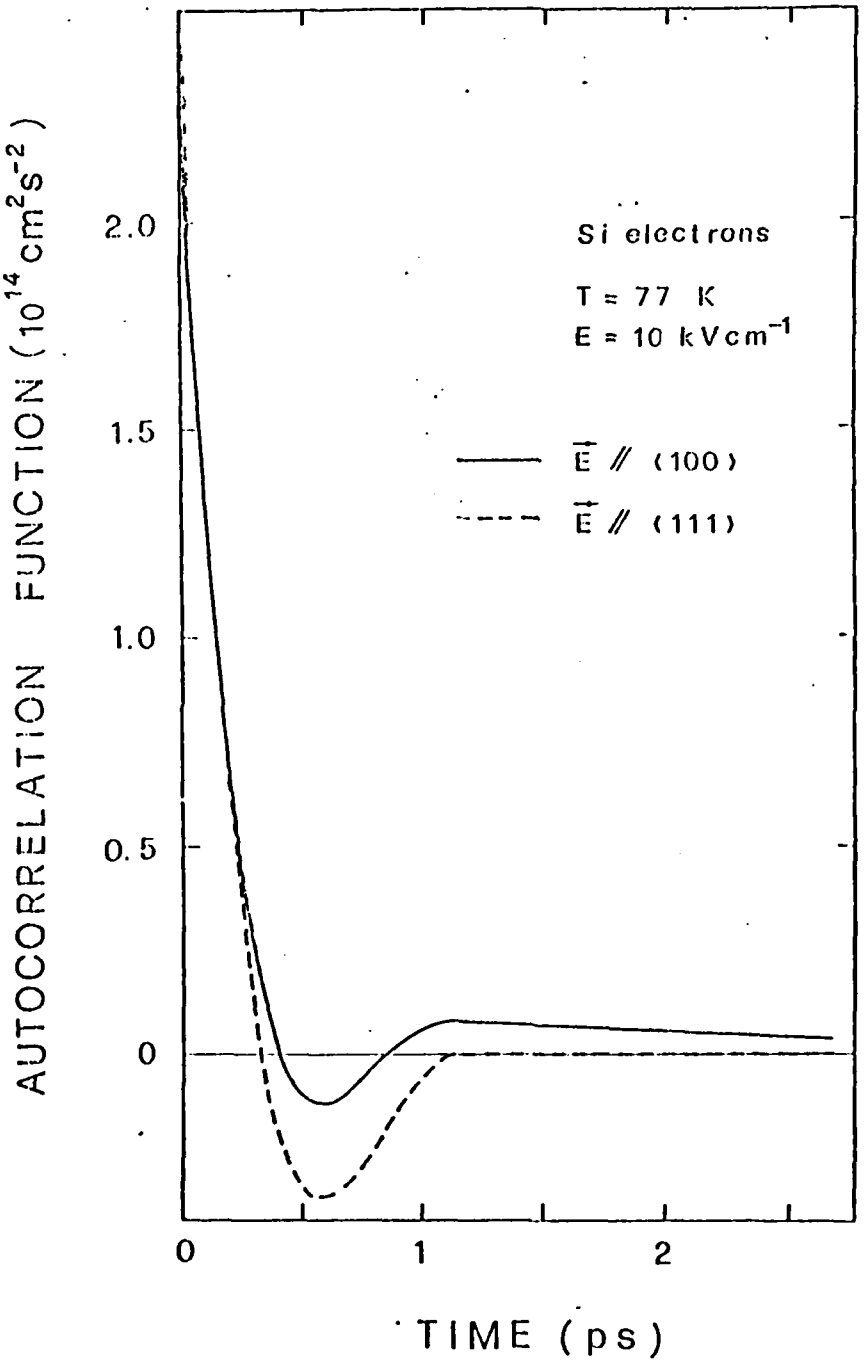
AUTOCORRELATION FUNCTION (10^{14} cm^{2}s^{-2})
2.0
1.5
1.0
0.5
0
0
1
2
TIME (ps)
Si electrons
T = 77 K
E = 10 kVcm^{-1}
$\vec{E}$ // (100)
$\vec{E}$ // (111)

FIG.4.1

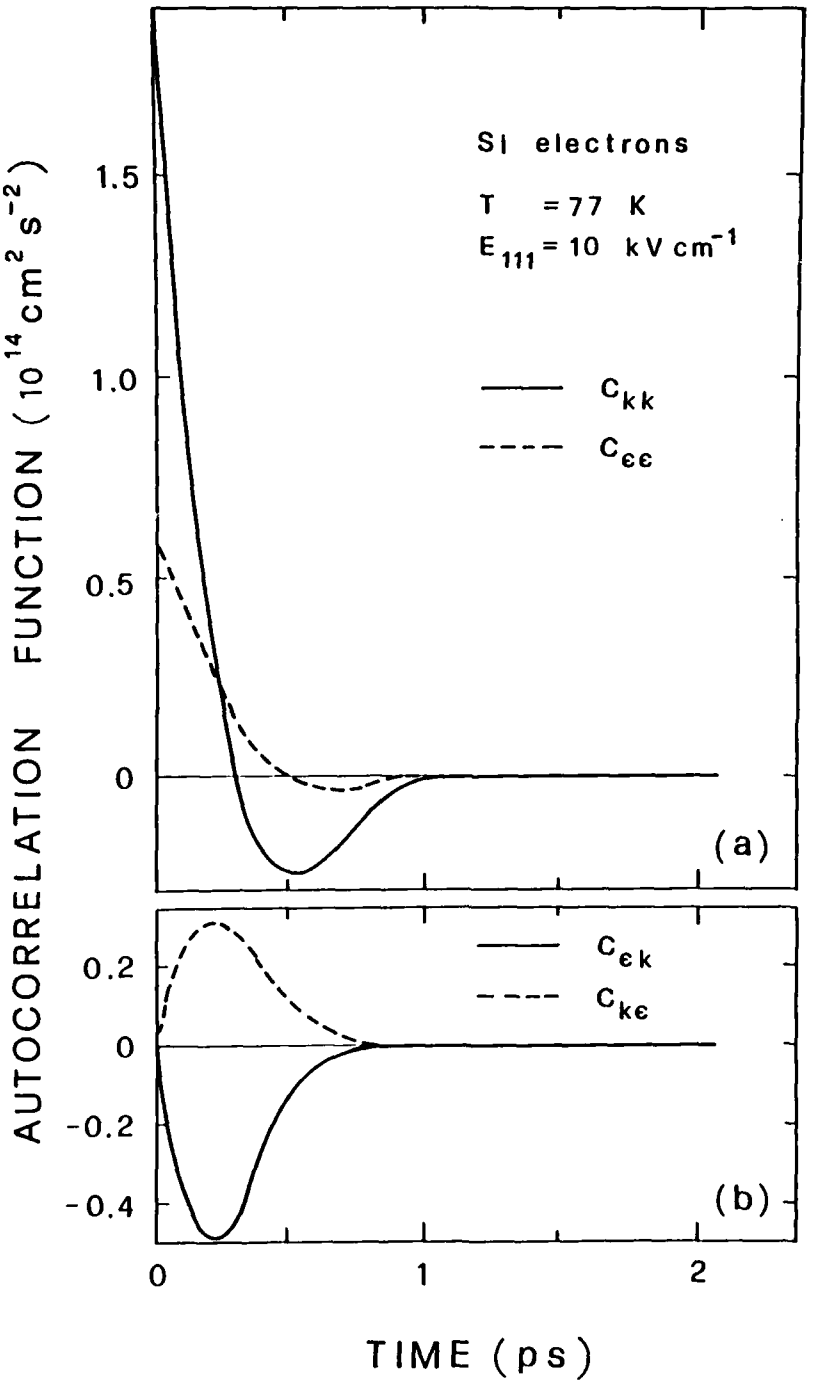
Si electrons
T = 77 K
E111 = 10 kV cm-1
Ckk
Cεε
Cεk
Ckε
(a)
(b)
AUTOCORRELATION FUNCTION (10^14 cm^2 s^-2)
TIME (ps)
1.5
1.0
0.5
0
0.2
-0.2
-0.4
0
1
2

FIG.4.2

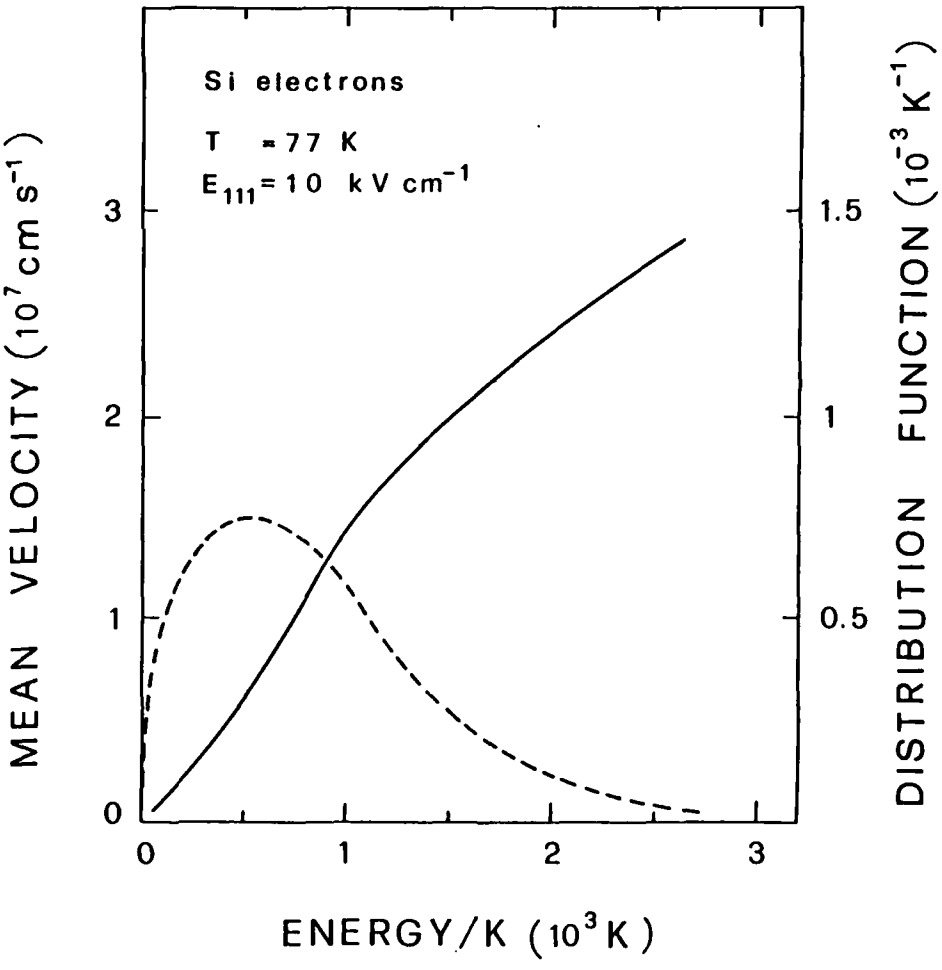
Si electrons
T = 77 K
E111 = 10 kV cm-1
MEAN VELOCITY (10^7 cm s^-1)
DISTRIBUTION FUNCTION (10^-3 K^-1)
ENERGY/K (10^3 K)
0
1
2
3
0.5
1.5

FIG.4.3

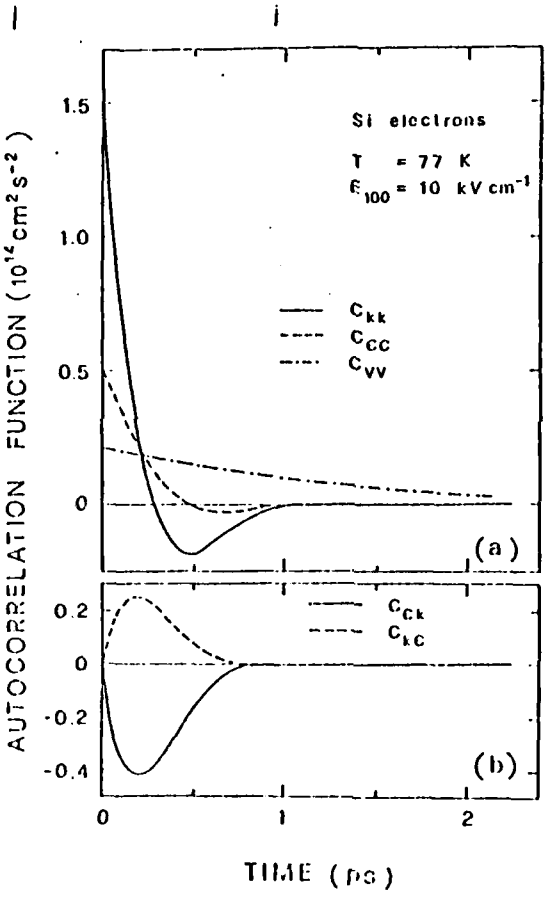
Si electrons
T = 77 K
E100 = 10 kV cm-1
Ckk
Ccc
Cvv
(a)
Cck
Ckc
(b)
AUTOCORRELATION FUNCTION (10^14 cm^2 s^-2)
TIME (ps)
1.5
1.0
0.5
0
0.2
0
-0.2
-0.4
0
1
2

FIG.4.4

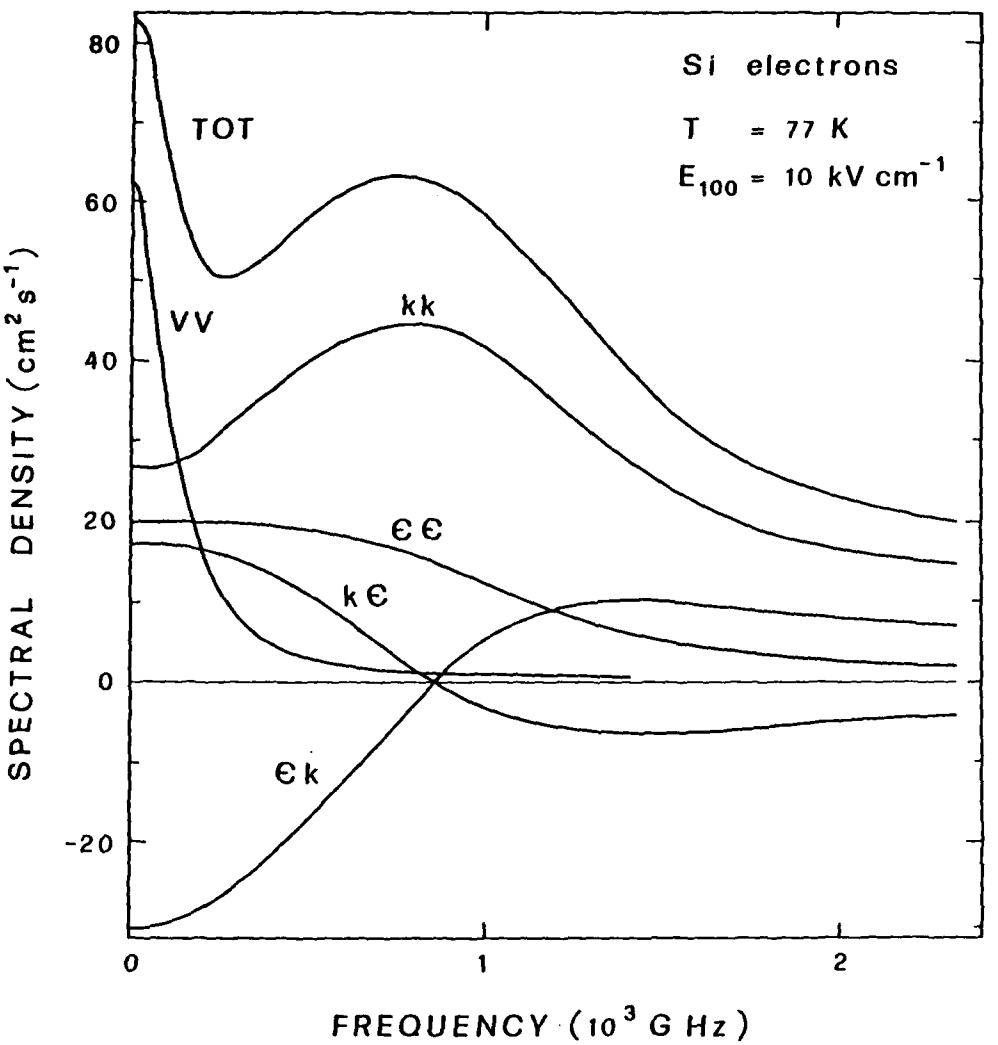
Si electrons
T = 77 K
E_{100} = 10 kV cm^{-1}
TOT
VV
kk
εε
kε
εk
80
60
40
20
0
-20
0
1
2
SPECTRAL DENSITY (cm^2 s^{-1})
FREQUENCY (10^3 G Hz)

FIG. 4.5

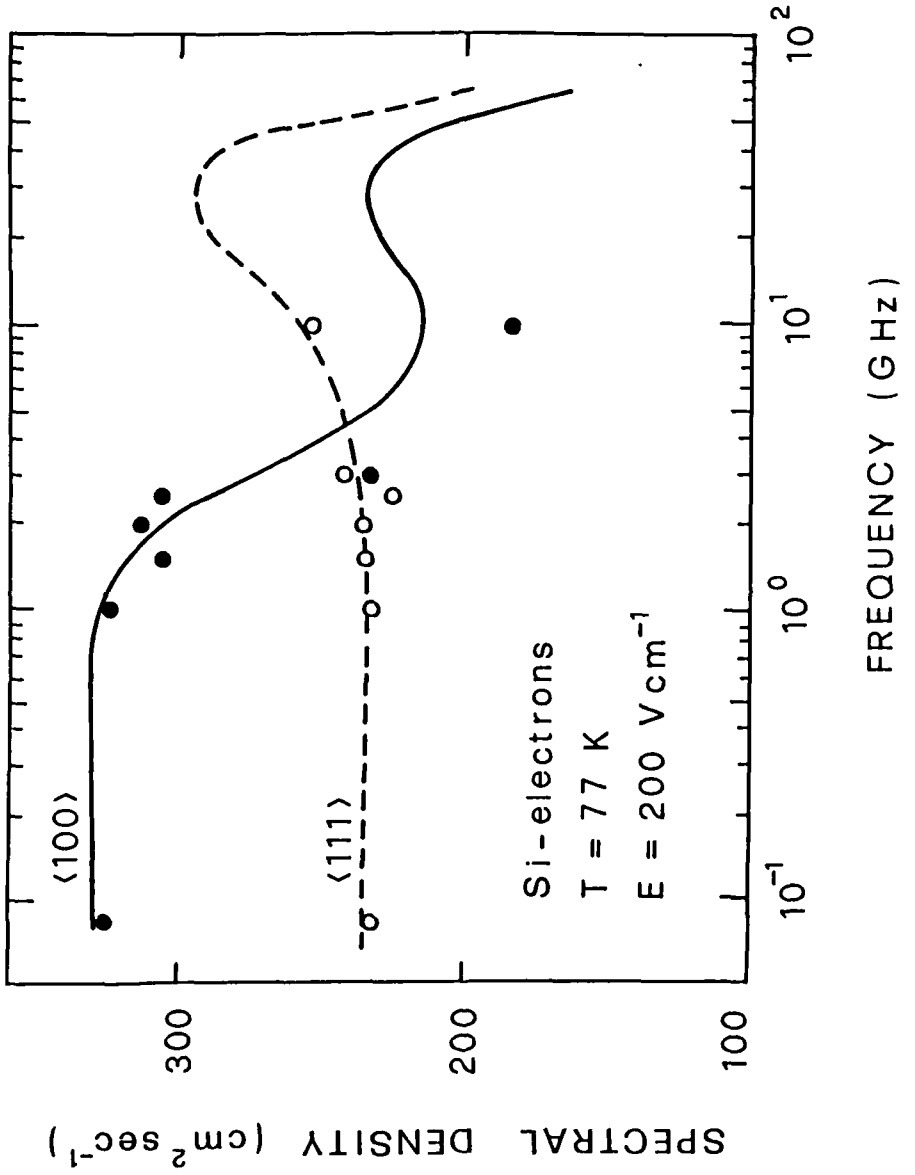
SPECTRAL DENSITY (cm^{2}sec^{-1})
300
200
100
10^{-1}
10^0
10^1
10^2
FREQUENCY (GHz)
⟨100⟩
⟨111⟩
Si-electrons
T = 77 K
E = 200 Vcm^{-1}

FIG. 4.6

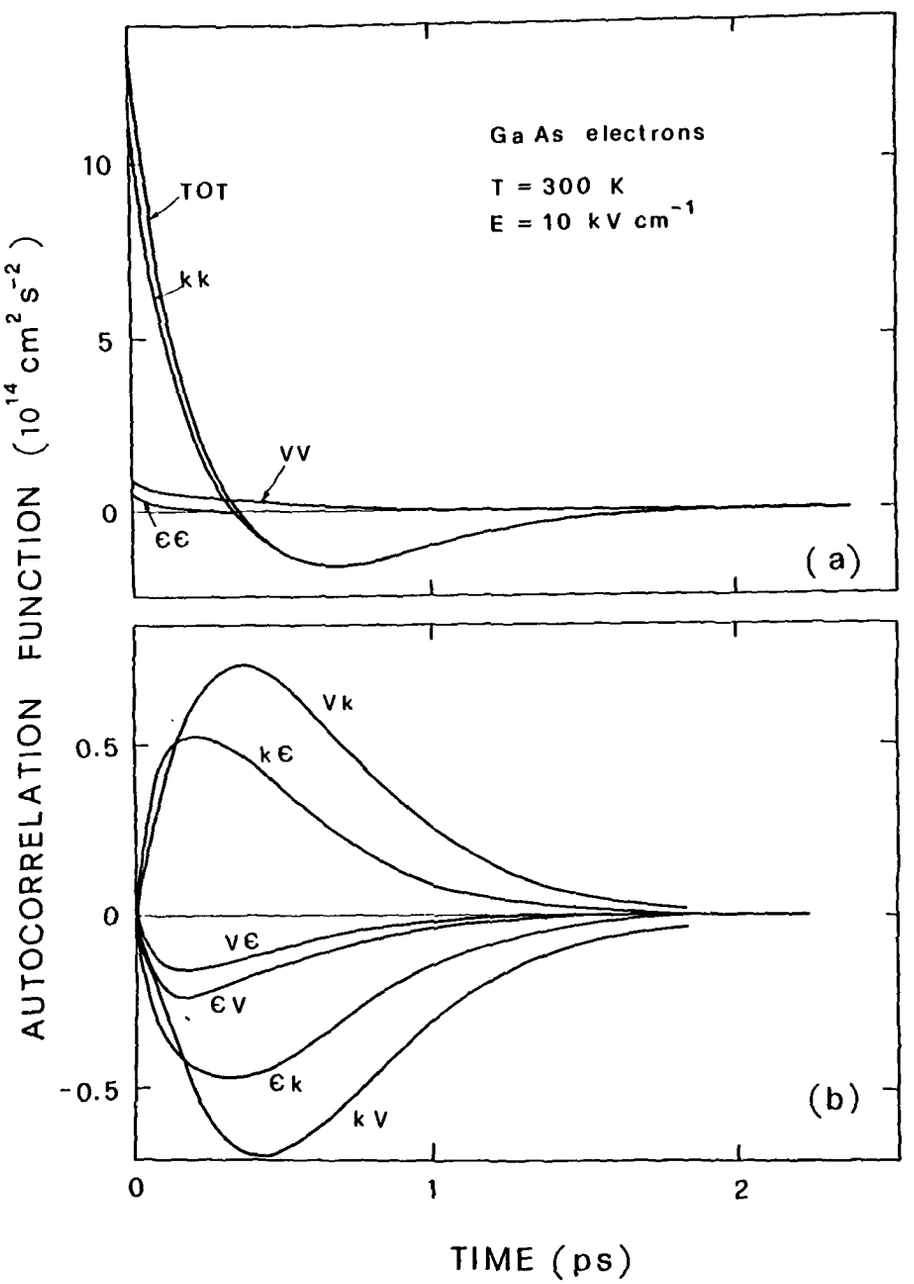
Ga As electrons
T = 300 K
E = 10 kV cm^{-1}
TOT
kk
VV
εε
(a)
Vk
kε
Vε
εV
εk
kV
(b)
AUTOCORRELATION FUNCTION (10^{14} cm^2 s^{-2})
TIME (ps)
10
5
0
0.5
-0.5
1
2

FIG. 4.7

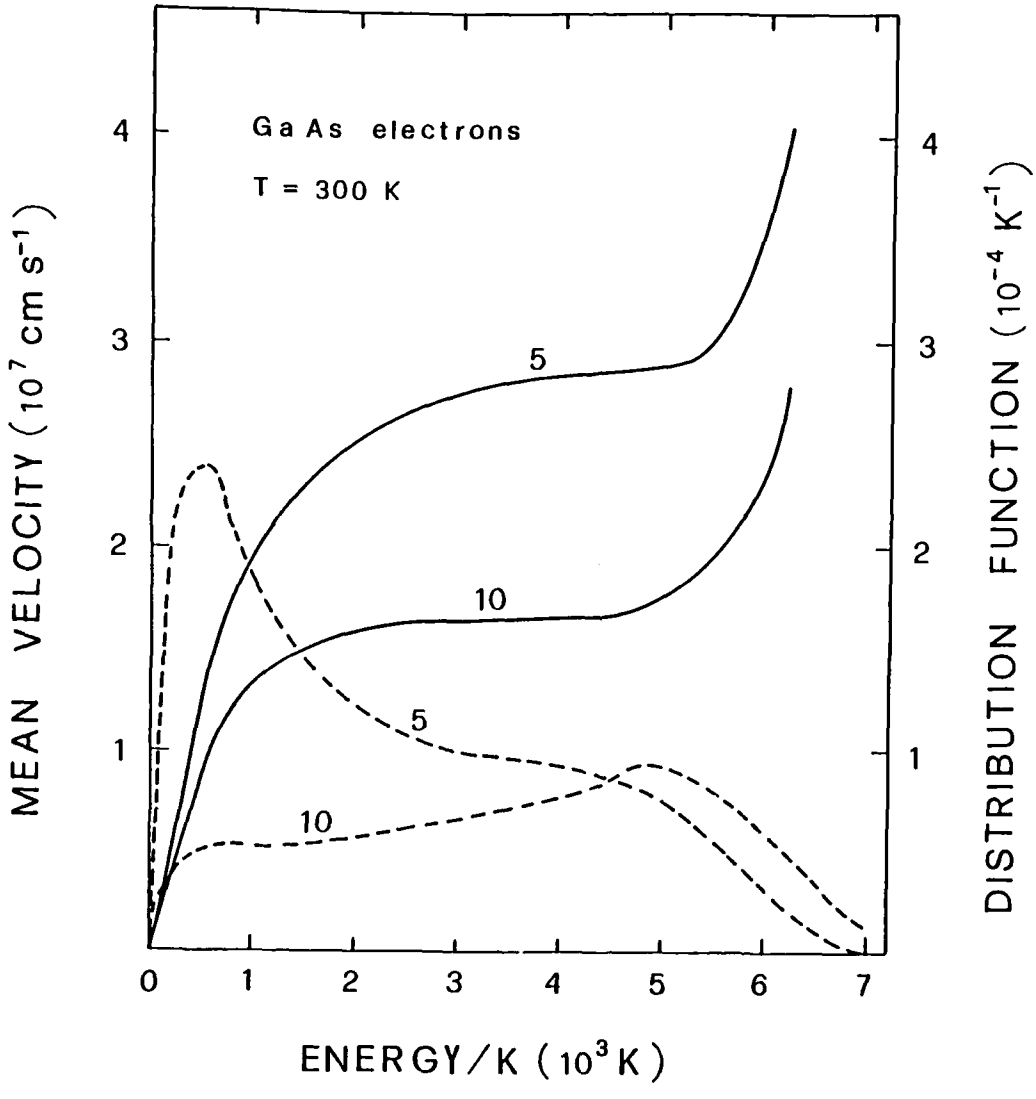
GaAs electrons
T = 300 K
5
10
5
10
MEAN VELOCITY (10^7 cm s^{-1})
DISTRIBUTION FUNCTION (10^{-4} K^{-1})
ENERGY/K (10^3 K)
0
1
2
3
4
5
6
7

FIG. 4.8

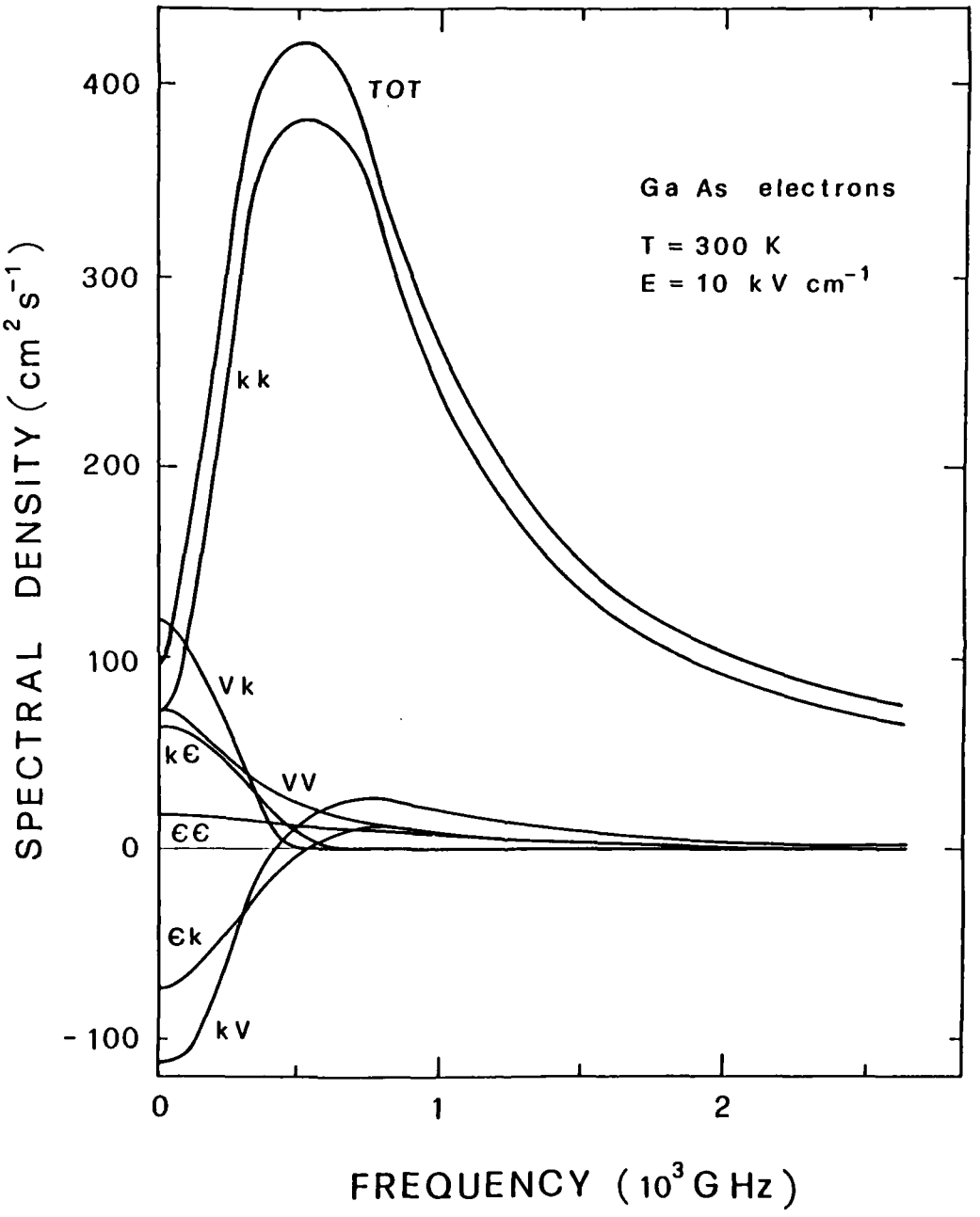
400
300
200
100
0
-100
TOT
kk
Vk
kϵ
VV
ϵϵ
ϵk
kV
Ga As electrons
T = 300 K
E = 10 kV cm^{-1}
SPECTRAL DENSITY (cm^{2}s^{-1})
0
1
2
FREQUENCY (10^3 GHz)

FIG. 4.9

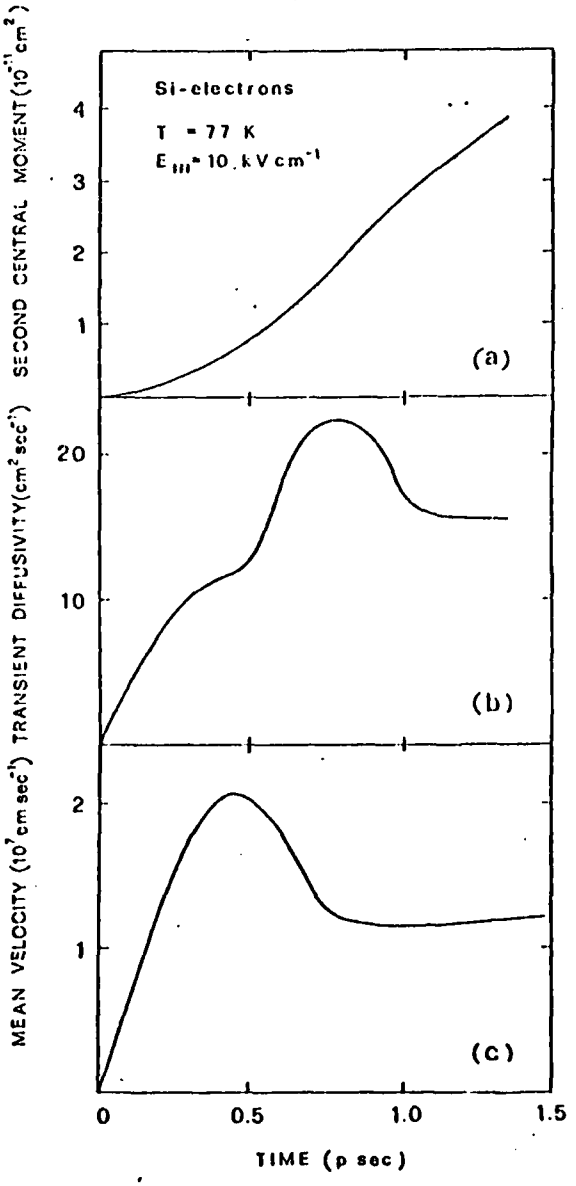
Si-electrons
T = 77 K
E_m = 10. kV cm^-1
(a)
(b)
(c)
4
3
2
1
20
10
2
1
0
0.5
1.0
1.5
TIME (p sec)
MEAN VELOCITY (10^7 cm sec^-1) TRANSIENT DIFFUSIVITY (cm^2 sec^-1) SECOND CENTRAL MOMENT (10^-11 cm^2)

FIG. 4.10

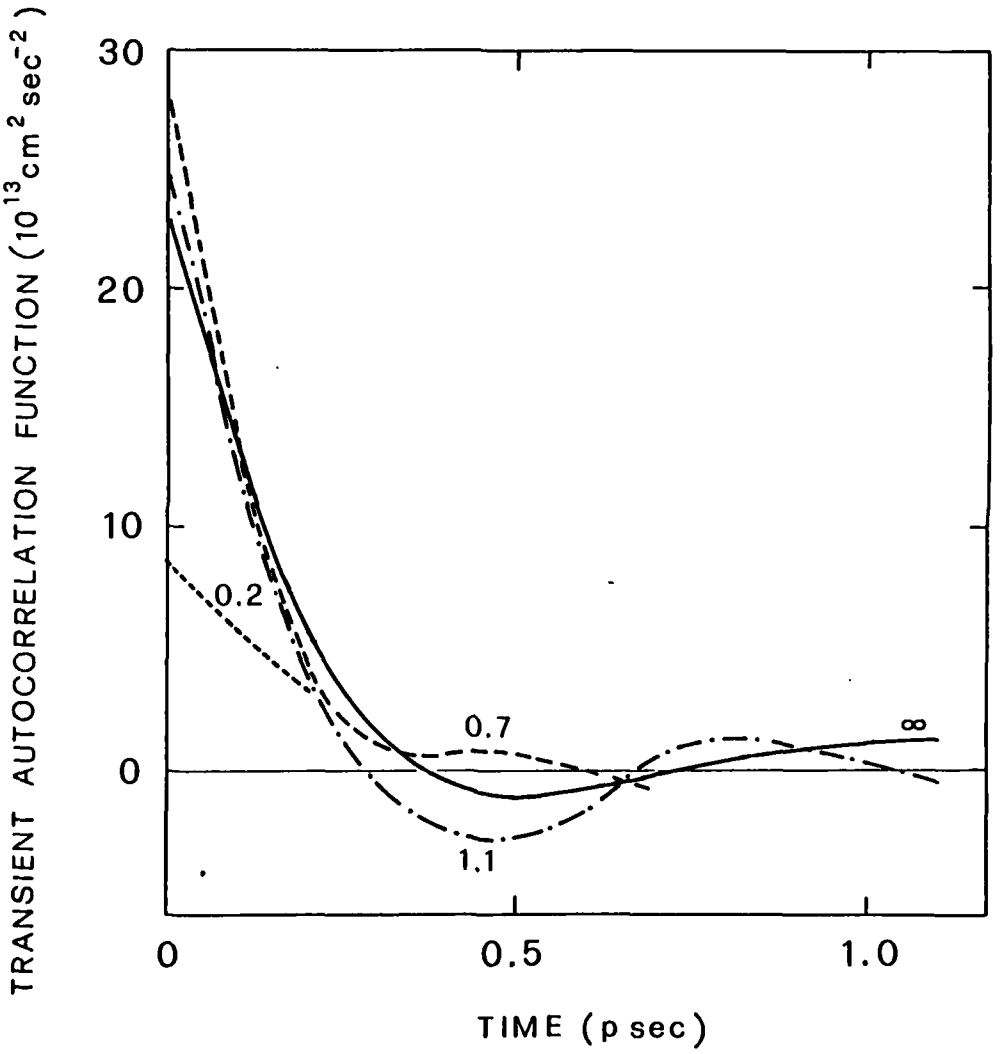
TRANSIENT AUTOCORRELATION FUNCTION (10^{13}cm^{2}sec^{-2})
30
20
10
0
0.2
0.7
1.1
∞
0
0.5
1.0
TIME (p sec)

FIG. 4.11

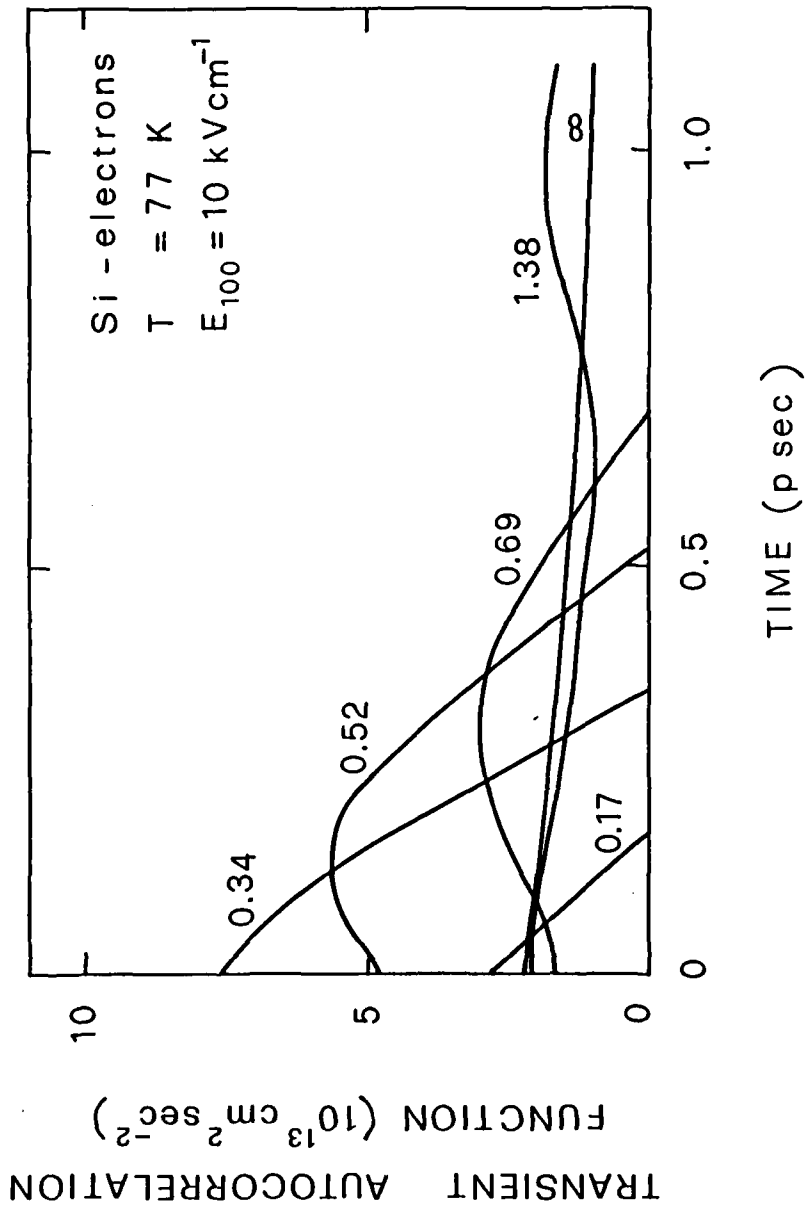
Si - electrons
T = 77 K
E_{100} = 10 kVcm^{-1}
0.34
0.52
0.69
1.38
8
0.17
0
0.5
1.0
TIME (p sec)
10
5
0
TRANSIENT AUTOCORRELATION FUNCTION (10^{13} cm^2 sec^{-2})

FIG. 4.12

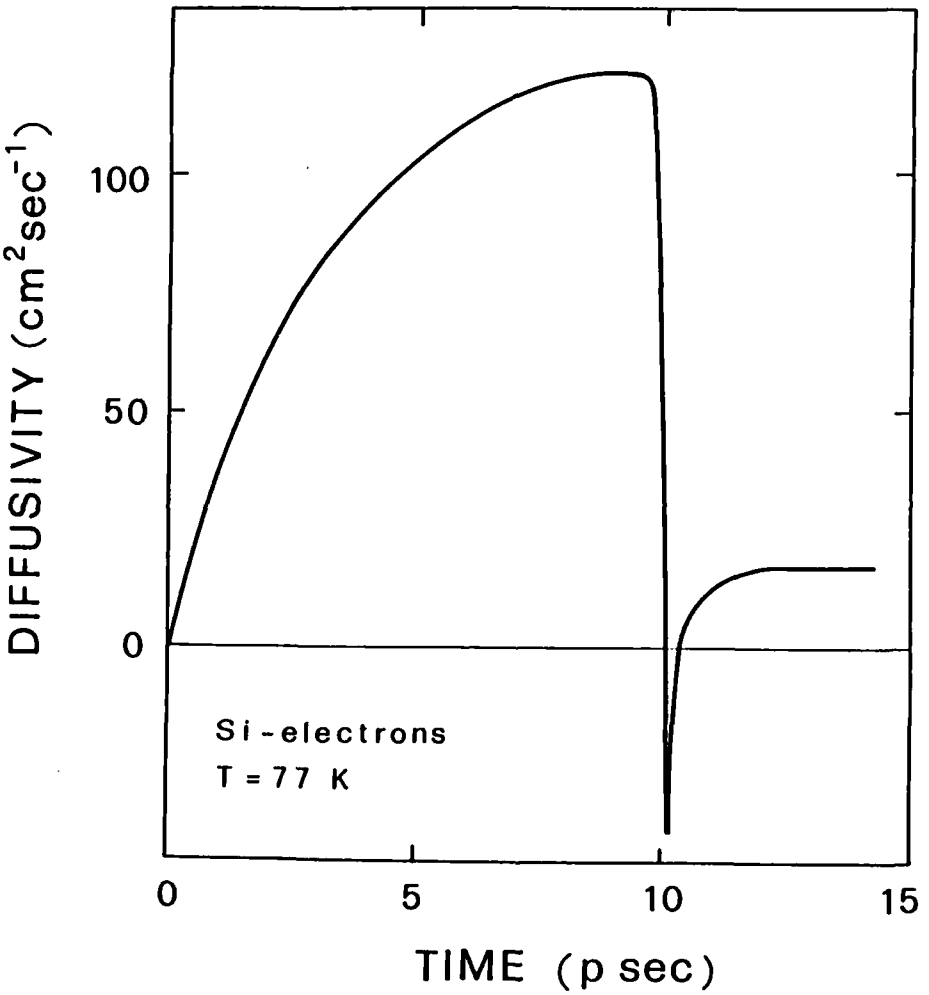
DIFFUSIVITY (cm^2sec^{-1})
100
50
0
Si - electrons
T = 77 K
0
5
10
15
TIME (p sec)

FIG. 4.13

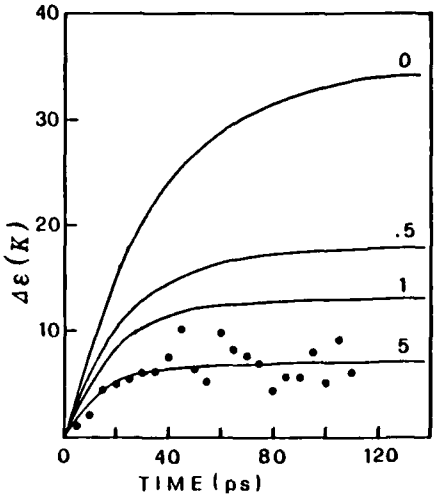

FIG. 4.14

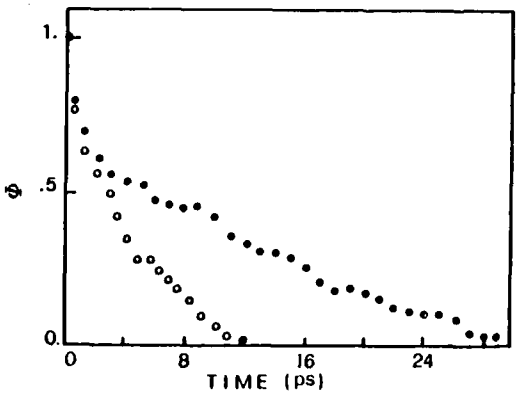

FIG. 4.15

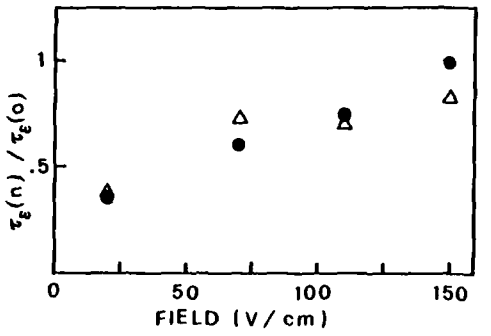

FIG. 4.16

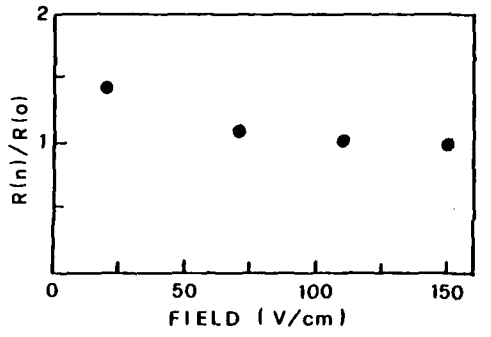

FIG. 4.17

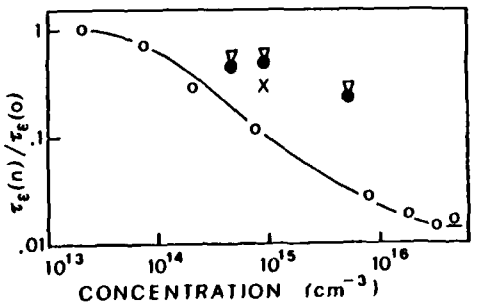

FIG. 4.18

5. CONCLUSIONS

The present report describes the research performed at the Department of Physics of the University of Modena for the ERO contract number DAJA45/83/C/0039 "Monte Carlo analysis of quantum transport and fluctuation in semiconductors".

As regards the analysis of velocity and energy fluctuations of charge carriers in semiconductors, the new results have been obtained and published (they are described in Chapter 4). In particular, both transient and steady-state regimes have been studied and the effect on noise of the various sources of fluctuations have been analised.

The effect of carrier-carrier interaction on energy fluctuations and therefore onenergy relaxation time has also been studied: the result is that a theoretical reduction of the energy relaxation time is indeed observed in the Monte Carlo simulation, but this reduction is not as strong as that observed in experiments.

As regard the extension of the Monte Carlo approach to study quantum transport, the research has required a careful

analysis of the state of the art, which has been presented in Chapter 2. A Monte Carlo method to solve integro-differential equations of the same type of transport equations has been developed. The possibility to apply such a method to the solution of the Liouville equation for quantum transport of electrons in a phonon field has been investigated. The set up of the numerical procedure for this case of practical importance is under development and requires further work.

END

FILMED

4-86

DTIC